Targeting fibroblastic reticular cells to modulate the immune response in the lymph node

Master's thesis in Cell biology

Pia Sundqvist, 41835
pia.sundqvist@abo.fi
Supervisors: Marko Salmi and Ruth Fair-Mäkelä
Åbo Akademi University supervisor: Cecilia Sahlgren
Study Program in Cell Biology
Faculty of Science and Engineering
Åbo Akademi University 2023

ÅBO AKADEMI UNIVERSITY
Master's thesis in Cell Biology
Pia Sundqvist, 2023
Targeting fibroblastic reticular cells to modulate the immune response in the lymph node

Abstract

Lymph nodes, in which foreign antigens are presented with the help of antigen-presenting cells to naïve lymphocytes, are important for the initiation of an immune response. Fibroblastic reticular cells (FRC) produce the extracellular matrix that forms the reticular conduit system, which provides structural support to the lymph node and sorts the soluble antigens based on their size into the lymph node parenchyma. During inflammation, the lymph node stroma is remodeled through stretching of the conduit system and proliferation of the FRCs to support the growing lymphocyte population. This thesis established a local FRC depletion model in the lymph nodes of CCL19-Cre x iDTR (CCL19-iDTR) mice and investigated the response of the lymph nodes with reduced FRC population during inflammation.

Our results indicate that the expression of Cre or Cre-inducible diphtheria toxin receptor (iDTR) does not affect the FRC number, and the CCL19-iDTR mouse model has the same initial amount of FRCs as wild-type mice. An injection of diphtheria toxin can reduce the FRC population by half in the draining popliteal lymph node in the CCL19-iDTR mouse model, but the depletion does not remain local. The draining popliteal lymph node can also respond to immunization after FRC depletion, but the expansion is not as effective as during normal circumstances. In conclusion, the FRCs regulate the immune response in the lymph node, but further studies are needed to determine their exact role during inflammation.

Keywords: CCL19-iDTR, fibroblastic reticular cells, inflammation, lymph node

Table of contents

Abbreviations

BEC	Blood vessel endothelial cell
CFA	Complete Freund's Adjuvant
CLEC-2	C-type lectin-like receptor 2
Col I	Collagen type I
DC	Dendritic cell
DT	Diphtheria toxin
DTR	Diphtheria toxin receptor
FDC	Follicular dendritic cell
FRC	Fibroblastic reticular cell
HEV	High endothelial venule
iDTR	Cre-inducible diphtheria toxin receptor
i.p.	intraperitoneal
LEC	Lymphatic endothelial cell
LTβR	Lymphotoxin-β receptor
LYVE1	Lymphatic vessel endothelial hyaluronan receptor 1
MHC	Major histocompatibility complex
MRC	Marginal reticular cell
MSM	Medullary sinus macrophage
OCT	Optimal cutting temperature
PECAM-1	Platelet endothelial cell adhesion molecule 1
PLVAP	Plasmalemma vesicle associated protein
PNAd	Peripheral node addressin
Prox1	Prospero homeobox protein 1
s.c.	subcutaneous
SCS	Subcapsular sinus
S1P	Sphingosine-1-phosphate
$S1P_1$	Sphingosine-1-phosphate receptor-1
SSM	Subcapsular sinus macrophage
Treg	T regulatory cell
VEGF	Vascular endothelial growth factor
VEGFR-3	Vascular endothelial growth factor receptor 3

1 Introduction

The immune system is vital for our health, and the non-leukocytic stromal cells play key roles in regulating the immune response. The immune cells migrate throughout our body via the blood and lymphatic vessels to find foreign antigens to target and eliminate. The lymphatic vessels connect the lymph nodes to each other and form the lymphatic system together with the other secondary lymphoid organs. Lymph nodes are dispersed in the periphery of our body, and the adaptive immune response is initiated here. Lymphocytes migrate into the lymph node to recognize foreign antigens. Foreign antigens, pathogens, and cancerous cells travel with the lymph to the lymph node. Upon encountering the antigen, the lymphocytes become activated and start eliminating the antigen to protect the host (Girard et al., 2012; Randolph et al., 2017).

The lymph node is divided into compartments, and the compartments are populated with different immune cells and non-leukocytic stromal cells. Immune cells and antigens use different routes to the lymph node. Antigens and dendritic cells (DC) migrate into the lymph node via lymphatic vessels, whereas naïve lymphocytes mainly migrate via the blood vasculature. The lymph draining into the lymph node is also filtered, and the lymph node actively regulates which molecules can enter into the lymph node parenchyma. Small soluble molecules are able to drain into the parenchyma through a specialized conduit system, while larger molecules are delivered with the migratory DCs. The fibroblastic reticular cells (FRC) produce the reticular conduit system, which gives structural support and directional guidance to migrating lymphocytes and regulates the size-selective entry of antigens into the lymph node. The conduit system and the FRCs span throughout the whole lymph node, but they are mainly enriched in the T cell zone in the paracortex. The FRCs are also important for the adaptive immune response and are constantly interacting with immune cells, ensuring that an immune response can be initiated (Acton & Reis e Sousa, 2016; Girard et al., 2012; Mueller & Germain, 2009).

The adaptive immune response is initiated when the foreign antigen is delivered to the lymph node and activates the naïve lymphocytes. Activated lymphocytes undergo clonal expansion, and the lymph node stroma is remodeled to accommodate the increase of lymphocytes as well as the lymph node expansion. During inflammation, the DCs bind to the FRCs inducing relaxation, leading to the stretching of the conduit system allowing the lymph node to expand. The FRCs also need to proliferate to allow the stroma to increase in size and support the growing number of lymphocytes. When the inflammation is resolved, the lymph node stroma will contract and return to homeostasis (Acton & Reis e Sousa, 2016; Thierry et al., 2019).

Model systems used for basic immunological research are often cell lines or mouse models, but other model systems are also used. Cell lines are usually too simple and lack the physiological complexity found *in vivo*. Among mammalian model systems, mouse models are the preferred model because of the availability of generation of genetically engineered mouse models and their similarity to humans. Discoveries in mouse models can be translated into humans, but species-specific differences need to be taken into account (Kim et al., 2020; Masopust et al., 2017). The aim of the thesis was to establish a local FRC depletion model in the draining lymph nodes with the CCL19-Cre x iDTR mouse model and to study how the lymph node responds to inflammation when the FRC population is reduced to develop a deeper understanding of the role of the FRCs in regulating the immune response.

2 Review of the Literature

2.1 Structure and function of the lymphatic system

The lymphatic system is one of the two major circulatory systems in the human body. It is a linear and open network connecting lymphatic vessels and secondary lymphoid organs to each other (Choi et al., 2012). Besides the lymphatic vessels, the lymphatic system includes the lymph nodes, Peyer's patches, spleen, tonsils, bone marrow, and the thymus (Mueller & Germain, 2009; Perez-Shibayama et al., 2019). The lymphatic vessels are found throughout the body, except the bones, brain, and spinal cord (Choi et al., 2012; Moore Jr. & Bertram, 2018). The blood capillaries leak out protein-rich fluid filtrates of plasma into the interstitial tissue space, where lymphatic capillaries absorb the fluid nonselectively and create lymph. The lymph is transported within the lymphatic vessels through lymph nodes, where immune cells encounter foreign antigens, and the adaptive immune response is initiated. The flow of the lymph is unidirectional returning fluids to the bloodstream via the thoracic duct connected to the subclavian vein to maintain the fluid balance (Moore Jr. & Bertram, 2018; Randolph et al., 2017). The three key functions of the lymphatic system are regulation of tissue fluid homeostasis, absorption and transportation of lipids and large molecules in the intestine, and conveying the traffic of immune cells and antigens to stimulate an adaptive immune response (Choi et al., 2012).

2.2 The lymph node

There are several hundreds of lymph nodes in the human body organized in clusters, whereas in mice the lymph nodes are organized in chains. The lymph nodes are dispersed throughout the periphery of the body. The afferent lymphatic vessels are the vessels that drain lymph into the lymph nodes, and the efferent lymphatic vessels are the ones that drain out the lymph from the lymph nodes. Lymph nodes harbor naïve lymphocytes that encounter the antigens and antigen-presenting cells, as well as activated, effector, and memory lymphocytes. The main role of the lymph node is to initiate an adaptive immune response against foreign invaders, such as bacteria and viruses. The lymph node is also important for maintaining the self-tolerance of the cells in the body (Girard et al., 2012).

2.3 Structure of the lymph node

The lymph node comprises of several structural regions, the cortex including the subcapsular sinus (SCS), paracortex and medullary sinus, and it is surrounded by a collagenous capsule (Figure 1). The majority of the cells in the lymph node are hematopoietic cells that recognize foreign antigens and become activated to create an immune response against them. The remaining cells in the lymph node are the stromal cells that can be divided into several subtypes based on their location, function, and phenotype. The main subtypes of stromal cells include blood vessel endothelial cells (BECs), lymphatic endothelial cells (LECs), and FRCs. Stromal cells constitute less than five percent of the cells in the lymph node and are essential for the function of the lymph nodes, because they give the lymph node its structure and contribute to the regulation of the immune response. Every structural region in the lymph node contains different lymphocytes and stromal cells, which helps with the function of that region (Girard et al., 2012; Grasso et al., 2021; Jalkanen & Salmi, 2020; Thierry et al., 2019).

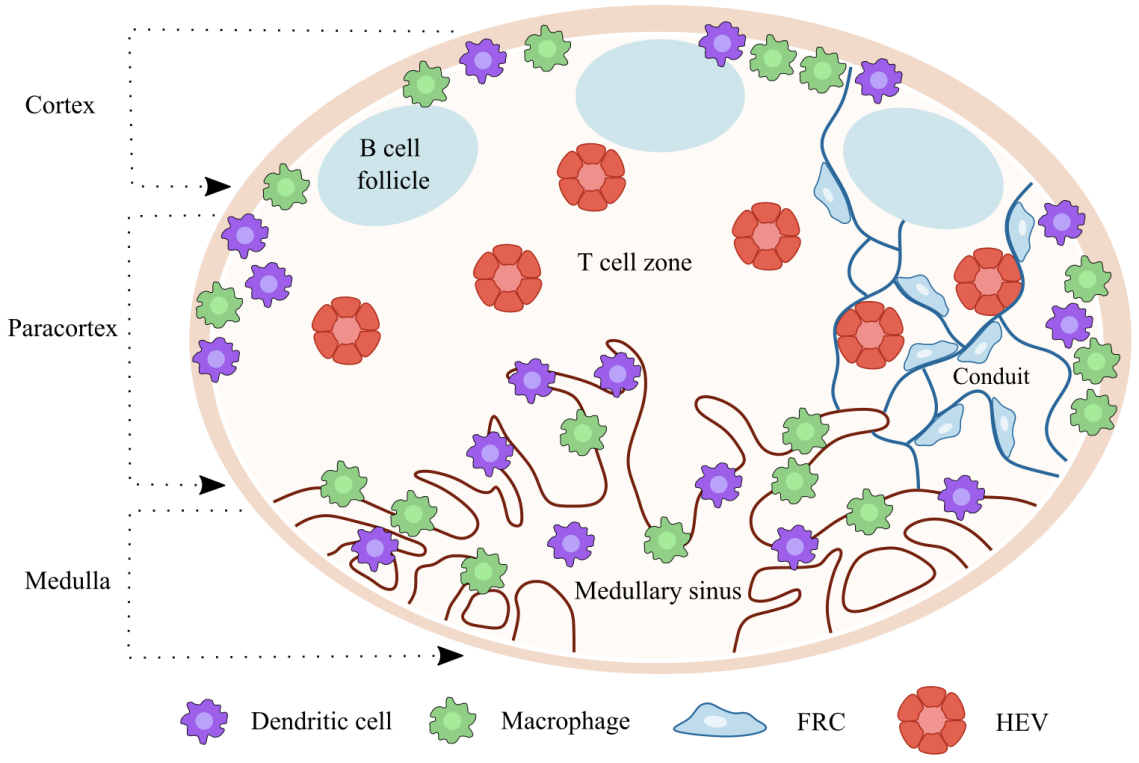

Figure 1. A schematic presentation of the organization of the lymph node showing the structural regions and main cellular components. The lymph node is divided into three main structural regions, the cortex, paracortex, and medulla. Fibroblastic reticular cell (FRC), high endothelial venule (HEV).

2.3.1 Reticular cells of the lymph node

One of the subtypes of the stromal cells in the lymph node is the reticular cell population derived from mesenchymal cells. The reticular cell population contains a majority of FRCs, in addition to follicular dendritic cells (FDC) supporting B cell follicles, marginal reticular cells (MRC) found in the SCS in lymph nodes, and other reticular cells. All reticular cells express podoplanin and are negative for CD31 and CD45, which separates them from endothelial and hematopoietic cells (Malhotra et al., 2013; Mueller & Germain, 2009). The different reticular cell populations are often collectively referred to as FRCs and not the different cell populations. Herein, the FRCs will collectively refer to all different cell populations, and the specific population will be mentioned if it is known.

The reticular cells can be found throughout the whole lymph node from the SCS to the medullary sinus. Single-cell RNA sequencing in mice revealed that reticular cells can be divided into nine subpopulations depending on their location in the lymph node (Rodda et al., 2018). The reticular subtypes form distinct microenvironmental niches in the lymph node (Figure 2) (Lütge et al., 2021). The two most well-characterized reticular cells, besides the FRCs, are the FDCs and MRCs. The expression of CXCL13 by the FDCs regulates the accumulation of the B cells and the formation of the B cell follicles (Ansel et al., 2000; Gunn et al., 1998). MRCs line the SCS and the outer surface of the B cell follicles and are involved in delivering antigens to the lymphocyte compartments in the lymph node and attracting B cells by secreting CXCL13 (Katakai, 2012; Roozendaal et al., 2009).

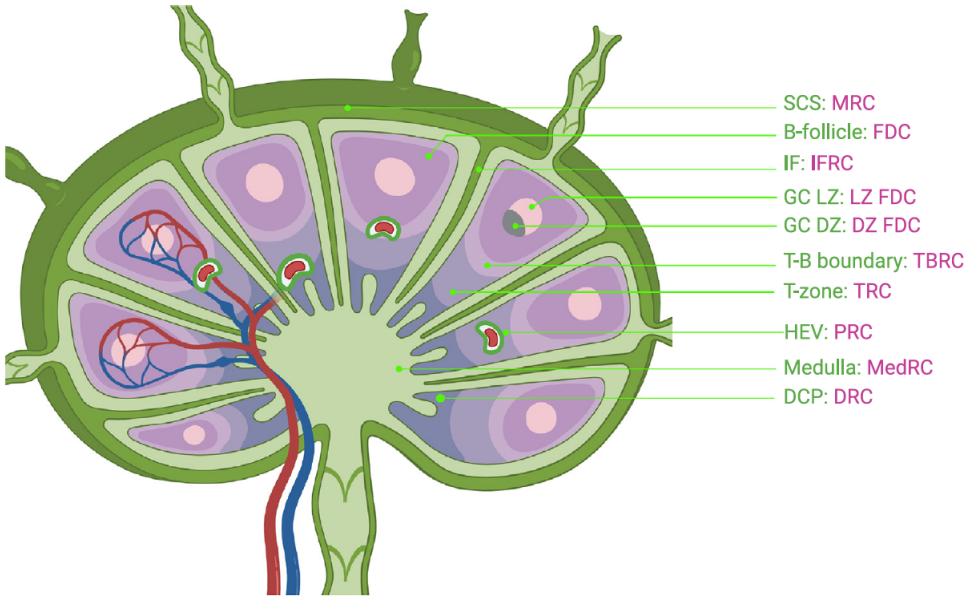

Figure 2. The reticular cell population forms distinct niches in the lymph node. Marginal reticular cells (MRC) line the SCS. Follicular dendritic cells (FDC) support the primary B cell follicles and the germinal centers. During germinal center reactions, FDCs form two subsets, one aligned to the light zone (LZ) and the other aligned to the dark zone (DZ). T-B border reticular cells (TBRC) are bordered by the T cell zone and B cell follicles, whereas interfollicular reticular cells (IFRC) are located between the B cell follicles. The T cell zone reticular cells (TRC) support the T cell zone, and the perivascular reticular cells (PRC) surround the veins and arteries. In the medulla are the medullary reticular cells (MedRC) situated, and the deep cortex periphery reticular cells (DRC) are located in the deep cortex periphery (Li et al., 2021).

2.3.2 Fibroblastic reticular cells

The FRCs produce the extracellular matrix that forms the conduit system, also called the reticular network, in the lymphoid compartment of the lymph node. The core of the conduit system consists of type I and II collagen that is surrounded by ER-TR7^{+} type VI collagen microfibrils, a basement membrane, and FRCs (Figure 3) (Schiavinato et al., 2021; Sixt et al., 2005). The Ccl19^{hi} T-zone reticular cells are the FRC population that ensheath the conduit. The conduit system provides structural support and regulates the entry of antigens into the lymph node. Furthermore, the conduit system gives directional guidance to the lymphocyte migration, so B cells migrate to the B cell follicles, and T cells migrate to the T cell zone along the conduit (Mueller & Germain, 2009; Rodda et al., 2018).

FRCs are continuously interacting with the other cell types in the lymph node ensuring that an adaptive immune response can be generated when necessary. FRCs express the

homeostatic chemokines CCL19 and CCL21, ligands for CCR7, which help the migration of naïve T cells and DCs across the HEVs and retain them in the paracortex (Förster et al., 1999; Luther et al., 2000). Survival of naïve T cells in the T cell zone is also supported by FRCs expression of IL-7 and CCL19 (Link et al., 2007). To support B cell survival, FRCs in the B cell follicles produce the B cell activating factor, BAFF, which is the main survival factor for mature B cells. When FRCs are depleted from the lymph node, the B cell follicles are reduced in size and lose their boundaries. The mice are also not able to produce proper humoral responses due to the reduction of B cells (Cremasco et al., 2014). Depletion of FRCs also reduces the naïve T cells and DCs (Denton et al., 2014). The expression of podoplanin by the FRCs is important for the DC migration on the conduit. When the C-type lectin-like receptor 2 (CLEC-2) expressed by the DCs interacts with the podoplanin on the FRCs, the DCs extend protrusions and start migrating along the conduit (Acton et al., 2012).

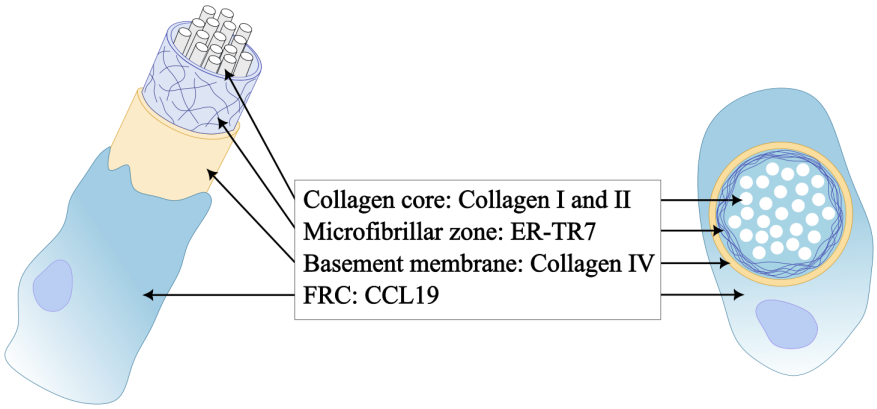

Figure 3. A schematic presentation of the conduit showing the main components and their markers. Figure adapted from Rantakari et al., 2015.

2.3.3 Lymphatics of the lymph node

The lymph node sinuses are lined with LECs. The lymph node capsule is penetrated by the afferent lymphatic vessels, which open up into the SCS. The SCS is a hollow space lined by two monolayers of LEC, one facing the capsule and the other facing the parenchyma of the lymph node. The LECs facing the capsule are called ceiling LECs, and those facing the parenchyma are called floor LECs. All LECs in the lymph node express platelet endothelial cell adhesion molecule 1 (PECAM-1, CD31), Prospero homeobox protein 1 (Prox1), and vascular endothelial growth factor receptor 3 (VEGFR-3), but depending on the location, lymph node LECs express additional lymphatic markers. The floor LECs are positive for lymphatic vessel endothelial hyaluronan receptor 1 (LYVE1), CCL21, and

MADCAM1, whereas the LECs in the ceiling express podoplanin and CCRL1 (Fujimoto et al., 2020; Jalkanen & Salmi, 2020; Ulvmar et al., 2014). Both LECs and FRCs produce IL-7, supporting the survival of naïve lymphocytes. LECs are the only stromal cell type to express CCL20, which is thought to contribute to the egress of activated lymphocytes from the draining lymph node (Liston et al., 2009; Malhotra et al., 2012). In addition, LECs also secrete sphingosine-1-phosphate (S1P), which guides the egress of lymphocytes from the lymph node (Pham et al., 2008). Lymph node LECs also express plasmalemma vesicle associated protein (PLVAP), forming diaphragms in a cartwheel-like structure that controls the transfer of molecules into the conduit (Rantakari et al., 2015).

With the help of single-cell RNA sequencing, six subtypes of human lymph node LECs have been identified (Takeda et al., 2019), whereas seven subtypes have been identified in murine lymph nodes. Humans and mice have five corresponding LEC subtypes with different anatomical locations in the lymph node. Many of the genes are conserved between the two species, such as CCRL1 and VEGFR-3, yet some genes are species-specific (Xiang et al., 2020). The floor LECs function as a barrier and mediate the transfer of macromolecules across the SCS into the parenchyma, whereas ceiling LECs separate the SCS from the fibrous capsule and the surrounding environment. Humans have transverse sinuses that create invaginations of LEC-lined SCS, forming open channels from the SCS to the medullary sinus. The cortical sinuses spin throughout the whole paracortex, where the egress of lymphocytes is initiated, and the lymphocytes are transported into the medullary sinuses. The medullary sinuses converge into the efferent lymphatic vessel leaving the lymph node with the lymph (Girard et al., 2012; Jalkanen & Salmi, 2020; Ulvmar et al., 2014).

2.3.4 Blood vasculature of the lymph node

The blood vasculature lumen in the lymph node is lined by BECs (Choi et al., 2012). The vasculature consists of arterioles, capillaries, venules, and specialized post-capillary venules called high endothelial venules (HEVs). The endothelial cells lining HEVs have a plump and cuboidal shape compared with the flat shape of endothelial cells lining other vessels (Girard & Springer, 1995). HEVs are predominately found at the boundary between the T and B cell zones in the cortical ridge (Katakai et al., 2004). During homeostasis, HEVs are the main entry sites for migrating naïve lymphocytes entering the lymph node, as well as other immune cells (Girard et al., 2012). The migration through the HEVs occurs in a multistep adhesion cascade where lymphocytes tether, roll, adhere, crawl, and transmigrate through the HEVs (Vella et al., 2021). Single-cell RNA sequencing has re-

vealed that endothelial cells in HEVs are heterogeneous. Depending on where the HEVs are found in the lymph node, genes important for lymphocyte migration are expressed differently (Veerman et al., 2019).

Many genes expressed by HEVs are not expressed by endothelial cells in other vasculatures, such as PNAd (peripheral node addressin), which is involved in lymphocyte migration (Streeter et al., 1988). The mature phenotype of HEVs is maintained by DCs, and if the DCs are depleted from the lymph node, HEVs will dedifferentiate into an immature state. This leads to reduced migration of lymphocytes into the lymph node. DCs express the ligands for the lymphotoxin-β receptor (LTβR) expressed by HEVs, and this LTβR signaling is required for the maintenance of HEVs' mature phenotype and lymphocyte homing (Moussion & Girard, 2011). FRCs also express LTβR, which regulates the vascular endothelial growth factor (VEGF) levels in the lymph node, thereby regulating HEVs and their proliferation (Chyou et al., 2008).

2.4 Immune cells

2.4.1 Lymphocytes

Lymphocytes reside in different compartments in the lymph node. B cells reside in the follicles in the cortex, where the B cell response occurs. Naïve B cells enter the lymph node mainly through the HEVs (Park et al., 2012), but a low number of B cells also migrate via the afferent lymphatic vessels to the lymph node (Hunter et al., 2016). B cells entering the lymph node through the HEVs migrate on the conduit toward the follicles (Bajénoff et al., 2006), following the CXCL13 chemokine gradient produced by the FDCs (Ansel et al., 2000). The FDCs produce a similar conduit system in the B cell follicles as the FRCs in the T cell zone. The FDCs capture and present unprocessed antigens to B cells, which are crawling on the network searching for antigens (Girard et al., 2012). Antigens can also be presented to B cells through interactions with follicular DCs and macrophages. B cells recognize both soluble and membrane-bound antigens (Batista & Harwood, 2009). After antigen recognition, B cells migrate to the T-B border in a CCR7-dependent manner to interact with cognate helper T cells (Garside et al., 1998; Okada et al., 2005). The interaction between the cells induces class-switch recombination, proliferation, and differentiation of the activated B cells into either plasmablasts, plasma cells, or memory B cells (Batista & Harwood, 2009; MacLennan et al., 1997).

T cells can migrate into the lymph node via the afferent lymphatic vessels or the HEVs with the blood circulation. $CD4^+$ effector and memory T cells migrate together with DCs via the afferent lymphatics, whereas naïve T cells migrate via the HEVs (Girard

et al., 2012; Mackay et al., 1990). T cells entering the lymph node via the HEVs migrate along the FRCs in the T cell zone. The FRCs secrete the chemokines CCL19 and CCL21, which bind to CCR7 expressed by the T cells. The binding between CCR7 and CCL19/21 regulates T cell migration in the lymph node stroma, in addition to the retention and accumulation of naïve T cells in the paracortical region of the lymph node (Bajénoff et al., 2006; Link et al., 2007; Pham et al., 2008; Worbs et al., 2007). Activated T cells are not retained in the lymph node by the CCL19 and CCL21 chemokines but by the downregulation of sphingosine-1-phosphate receptor-1 ($S1P_1$) (Denton et al., 2014). A naïve T cell's chance of encountering its cognate antigen increases since DCs also reside in the paracortex where they present foreign antigens to lymphocytes (Girard et al., 2012). For both $CD4^+$ and $CD8^+$ T cells, the initial activation occurs in the T cell paracortex after encountering the foreign antigens. The cells migrate into the interfollicular region or medullary sinus, which is rich in antigens increasing the chance of cellular interactions and priming of the T cells. The T cell migration into the different regions in the lymph node is CXCR3-dependent and is controlled by its ligands, CXCL9 and CXCL10, expressed by DCs and FRCs. After $CD4^+$ and $CD8^+$ T cells have encountered their cognate antigen, they mature into different subtypes of effector or memory cells (Duckworth & Groom, 2021; Groom, 2019).

2.4.2 Macrophages

Macrophages can be found throughout the whole lymph node, but are mainly located within the lymphatic sinuses. The lymph node macrophages are divided into five subsets: subcapsular sinus macrophages (SSM, $CD169^+$, $F4/80^-$), medullary sinus macrophages (MSM, $CD169^+$, $F4/80^+$), medullary cord macrophages ($CD169^-$, $F4/80^+$), macrophages in the germinal center ($CD68^+$, $CX3CR1^+$, $MERTK^+$), and T cell zone macrophages ($CD64^+$, $CX3CR1^+$, $MERTK^+$) (Bellomo et al., 2018).

The SSM line the floor of the SCS, overlaying the B cell follicles in the cortex. A part of the macrophages project into the SCS lumen meanwhile also protruding into the underlying follicles with long processes. Immune complexes and viruses are retained on the surface of the SSM for presentation to naïve follicular B cells, although SSM have limited endocytic activity and low degradative capacity (Junt et al., 2007; Phan et al., 2007, 2009). MSM are in contrast highly endocytic and can efficiently take up antigens in the medulla and interfollicular region between the B cell follicles for clearance of pathogens (Gray & Cyster, 2012; Phan et al., 2009). T cell zone macrophages reside in the T cell area of the paracortex where they clear apoptotic cells. *In vitro* studies have reported that

T cell zone macrophages crosstalk with FRCs and regulate their homeostasis (Baratin et al., 2017).

2.4.3 Dendritic cells

DCs are antigen-presenting cells that are indispensable for the initiation of adaptive immune responses. They also capture and present self-antigens to T cells to maintain peripheral tolerance. In the lymph node, there are two types of DCs, resident, i.e., classical DCs, and migratory DCs (Itano & Jenkins, 2003; Worbs et al., 2017). DCs migrate from tissues into lymph nodes via afferent lymphatic vessels using amoeboid movement that is integrin-independent (Lämmermann et al., 2008). On the afferent side of the lymph node, DCs migrate into the parenchyma by crossing the SCS floor at the interfollicular region (Braun et al., 2011). The migration of tissue-resident DCs is guided by the CCR7 ligands CCL19 and CCL21 expressed by the FRCs (Förster et al., 1999; Link et al., 2007). DCs express CLEC-2, which binds to podoplanin expressed by FRCs and LECs. The interaction between the molecules is required for the DCs to enter the lymphatics and migrate into the lymph node parenchyma with the help of extending protrusions (Acton et al., 2012).

Antigens can be presented to T cells by both resident and migratory DCs in the T cell zone. The difference is that migratory DCs bring the antigen with them from the periphery, and resident DCs take up the antigen in the lymph node (Acton & Reis e Sousa, 2016). Resident DCs are in direct contact with the conduit system and are able to take up and process soluble antigens from the conduit. However, migratory DCs reside between the T cells because they have already acquired the antigen in the periphery and do not need to sample it from the conduit (Sixt et al., 2005). Antigens are often acquired in peripheral tissues such as the skin, where skin-resident dermal DCs and Langerhans cells constantly migrate from the skin to the lymph node. During inflammation, their migration via lymphatic vessels increases for the presentation of antigens to naïve T cells to initiate adaptive immune responses (Itano et al., 2003; Randolph et al., 2005). Both migratory and resident DCs localize in different areas of steady-state lymph nodes, creating compartments with distinct functions (Gerner et al., 2012).

2.5 Lymph node function

The primary function of the lymph node is to mount an adaptive immune response against foreign antigens. The antigens can gain entrance to the lymph node within the migratory DCs or as free lymph-borne antigens. The lymph-born antigens can migrate across the

SCS through several different pathways. Another crucial function of the lymph node is maintaining peripheral tolerance and preventing autoimmunity (Jalkanen & Salmi, 2020).

2.5.1 Routes of antigen transport

Foreign antigens are delivered to the lymph node with the afferent lymph. In the SCS, soluble lymph-born antigens with a molecular weight under 70 kDa are directly delivered with the conduit system to the parenchyma and lumen of the HEVs. The collagen core of the conduit system limits the size of the molecules entering the conduit to a molecular weight under 70 kDa. The size limitation is due to the collagen core only physically allowing molecules with a hydrodynamic radius of approximately 5-6 nm, equal to a molecular weight $<$ 70 kDa, to freely enter the conduit (Gretz et al., 2000; Sixt et al., 2005). Molecules with higher molecular weight ($>$ 70 kDa) will not enter the conduit but are instead rapidly transported from the SCS into the lymph node parenchyma via LEC-mediated transcytosis (Kähäri et al., 2019). The separation of molecules in the lymph node SCS is at least partially controlled by PLVAP (Plasmalemma vesicle-associated protein), which forms sieve-like diaphragms in the LECs that overlay the openings into the conduit. Large antigens with a molecular weight of up to 500 kDa can enter the conduit system in mice deficient of PLVAP. The enhanced access to the parenchyma increases the uptake of large antigens by DCs and macrophages. Lymphocytes also increase their migration through the LEC floor into the parenchyma in the absence of PLVAP (Rantakari et al., 2015).

Small antigens enter the B cell follicles passively through the conduit system. The reticular network begins from the SCS and extends into the B cell follicle, and resembles the conduit structures found in the paracortex. B cells can, similarly to DCs, extend pseudopods and be in direct contact with the conduit. Thus, sampling antigens from the conduit leads to more rapid activation of B cells (Roozendaal et al., 2009). Immune complexes, i.e., complexes formed by antibodies binding to large antigens, are captured from the afferent lymphatic flow on the surface of the floor lining SSM in the SCS. Follicular B cells in close proximity to the SCS, capture the immune complexes from protrusions extending from the macrophages into the follicles in a complement receptor-dependent manner. The complexes are transported with the follicular B cells to the FDCs. B cells can also directly take up their cognate antigen from the SSM through their B cell receptor and then migrate to the T-B border to interact with the cognate T cell (Phan et al., 2007, 2009). Draining lymph nodes receive pathogens from peripheral tissues with the lymph. The SSM lining the SCS floor capture viruses and thus prevent systemic dissemination of

the pathogen. The viruses are transferred from the SCS with the help of SSM to the B cell follicles, initiating humoral immune responses (Junt et al., 2007).

Peptides derived from large antigens can be presented to naïve T cells in two waves. Resident DCs can take up antigens in the draining lymph nodes and present the antigen to naïve T cells before migratory DCs arrive. Migratory DCs phagocytes peptides in the periphery, and approximately 12 hours after the ingestion, the DCs arrive at the lymph node (Itano & Jenkins, 2003; Itano et al., 2003). The FRCs are the primary cell type that covers the conduit system, but about 10% is covered by macrophages and resident DCs. Of the resident DCs, 60-80% of them are in close contact with the conduit system. The resident DCs are able to physically take up and process soluble antigens from the conduit and initiate immune responses before migratory DCs have migrated into the lymph node from the periphery (Hayakawa et al., 1988; Sixt et al., 2005).

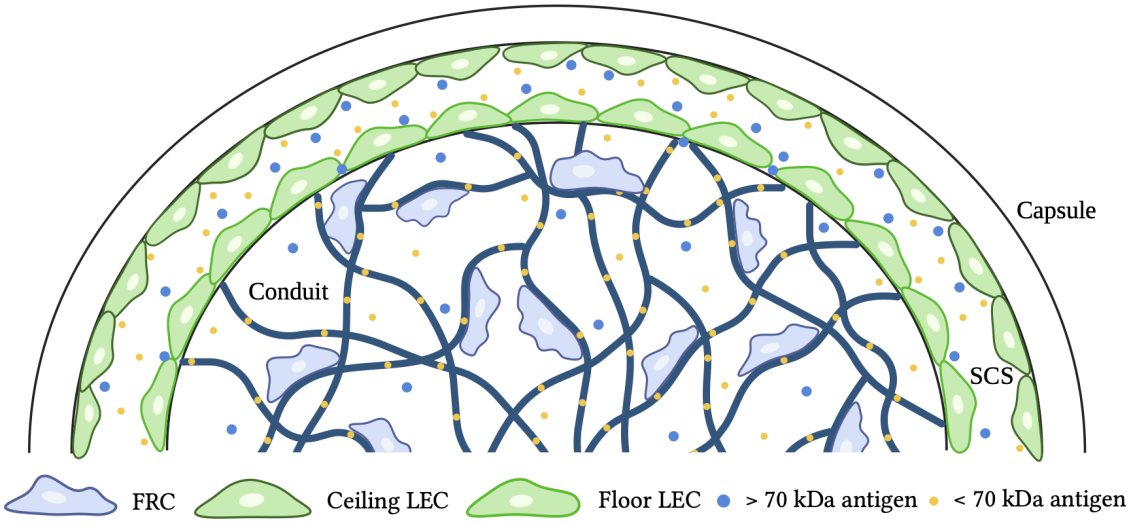

Figure 4. Antigens entering the lymph node are sorted based on their molecular size. Small antigens with a size $<$ 70 kDa enter directly into the conduit system, meanwhile, larger antigens $>$70 kDa are rapidly transported into the lymph node parenchyma via transcytosis through the floor lymphatic endothelial cells (LEC) in the subcapsular sinus (SCS). Fibroblastic reticular cell (FRC), figure created with BioRender.

2.5.2 Role of stromal cells in peripheral tolerance

Lymph node stromal cells have a role in peripheral tolerance, thereby preventing autoimmunity against self-antigens. The stromal cells are able to present antigens on major histocompatibility complex class I (MHCI) and class II (MHCII) to T cells, inducing their proliferation, even though DCs are the professional antigen-presenting cells. One of the

requirements for functional activation of T cells is signaling through co-stimulatory receptors. Stromal cells lack these co-stimulatory molecules, therefore T cells are unable to mature into effector cells, leading to their apoptosis (Hirosue & Dubrot, 2015).

Antigens can be intracellular or extracellular. Intracellular antigens form a complex with MHCI and are presented to $CD8^+$ T cells, whereas extracellular antigens are presented on MHCII to $CD4^+$ T cells (Hirosue & Dubrot, 2015). FRCs, LECs, and BECs express a range of peripheral tissue-restricted antigens on MHCI, directly presented to naïve $CD8^+$ T cells leading to the deletion of self-reactive T cells. Each subtype has its own characteristic antigen display in different anatomical locations (Cohen et al., 2010; Fletcher et al., 2010; Hirosue & Dubrot, 2015). For example, the only lymph node stromal subtype to express melanocyte-specific protein tyrosinase is LECs (Cohen et al., 2010), and FRCs are the only subtype that express Mlana (Fletcher et al., 2010). To further prevent autoimmunity, LECs express high levels of the inhibitory molecule PD-L1, upregulating the expression of PD-1 on $CD8^+$ T cells. This leads to the deletion of self-reactive T cells and maintenance of tolerance (Tewalt et al., 2012).

MHCII expression on stromal cells is highly regulated by the class II transactivator, in comparison to MHCI, which is expressed by most nucleated cells (Reith et al., 2005). $CD4^+$ T cells' survival can be limited by the stromal cells BECs, LECs, and FRCs acquiring self-peptide:MHCII complexes from DCs by direct cell-cell contact or within DC-derived exosomes. During steady-state, the level of MHCII expressed by the stromal cells is regulated by the number of DCs present in the lymph node (Dubrot et al., 2014). LECs can synthesize the MHCII molecules themselves, but LECs are not able to present the antigens to $CD4^+$ T cells because molecules are missing for the antigen loading pathways. Instead, LECs can function as a reservoir for antigens and transfer self-antigens to DCs, which present them to $CD4^+$ T cells, inducing T cell anergy (Rouhani et al., 2015). However, both BECs and FRCs express the molecules that LECs lack for antigen loading, but it is uncertain if they only function as antigen reservoirs or if they can directly regulate T cell tolerance (Malhotra et al., 2012). T regulatory cells (Treg) are important for the induction of peripheral tolerance and the prevention of autoimmunity. In the lymph node, Tregs are maintained by the presence of MHCII expressed by the stromal cells (Baptista et al., 2014). $CD4^+$ T cells can be converted into Tregs upon self-antigen presentation by FRCs and LECs. The conversion is IL-2 dependent and limits the generation of autoreactive T follicular helper cells and the humoral response (Nadafi et al., 2020).

2.6 Inflammation-induced changes in the lymph node

During inflammation, foreign antigens are delivered to the draining lymph node, and the adaptive immune response is initiated. The naïve T cells become activated when encountering the cognate antigen presented by the DCs, and the T cells undergo clonal expansion. This leads to the production of a large number of T cells recognizing the antigen, which helps with the elimination of the pathogen-derived antigen. B cells differentiate into plasma cells upon antigen recognition and start producing antibodies against the specific antigen (Acton & Reis e Sousa, 2016; Batista & Harwood, 2009). Following inflammation, lymphocyte egress is shut down, and the lymphocytes are retained in the lymph node to increase the probability of encountering their cognate antigen. CD69 expressed by T cells physically interacts with $S1P_1$, and the complex is internalized, limiting the egress of the lymphocytes. After three days, the expression of $S1P_1$ is regained by the T cells, and they are able to egress from the lymph node (Cyster & Schwab, 2012). The lymph node expands up to 20-fold to accommodate the influx of immune cells and trapping of lymphocytes, and the stromal network is remodeled to support the expansion (Thierry et al., 2019).

Immediately after the initiation of the adaptive immune response, the primary feeding arteriole is expanded to increase the entry of activated DCs (Soderberg et al., 2005), and the HEVs are multiplied to facilitate the increased migration of lymphocytes into the parenchyma. DCs regulate the growth of the vascular compartment (Webster et al., 2006) through signaling via LTβR ligands, increasing the production of VEGF. VEGF is produced by the FRCs surrounding the vessels, providing the signal for the proliferation of BECs (Chyou et al., 2008). A couple of days after the adaptive immune response starts, the afferent lymphatic vessels are impaired, and the afferent lymph factors are reduced in the lymph node. Consequently, the HEVs are dedifferentiated into an immature state and downregulate the expression of HEV-specific markers. The lymphatic vessel function is recovered approximately one week after the inflammation, and the HEVs recover their mature state (Liao & Ruddle, 2006). The permeability of HEVs is increased during inflammation, and platelets leak out into the lymph node parenchyma. In the parenchyma, the platelets encounter the perivascular reticular cells around the HEVs. CLEC-2 on the platelets interacts with podoplanin expressed by the perivascular reticular cells, causing S1P release from platelets. S1P signaling promotes upregulation of VE-cadherin on HEVs, maintaining HEV adherens junctions and preventing further leakage (Herzog et al., 2013). The vascular-stromal growth during inflammation can be divided into two distinct phases, an initiation phase and a subsequent expansion phase. The initiation phase is

lymphocyte-independent but requires $CD11^+$ cells, such as DCs, to upregulate the proliferation of the vasculature and stroma in the lymph node. The subsequent expansion phase is lymphocyte-dependent and expands the vascular-stromal compartment (Chyou et al., 2011).

Under homeostatic conditions, podoplanin expressed on FRCs controls the contraction of actomyosin in the conduit network. During inflammation, CLEC-2 on DCs binds to podoplanin, and the podoplanin expression is blocked on the FRCs, thereby inhibiting contraction. The relaxation of the FRCs leads to the stretching of the conduit network, and the lymph node can expand. The expansion of the lymph node also contributes to enhanced activation and proliferation of T cells (Acton et al., 2014; Astarita et al., 2015). CCR2-dependent monocytes and CCR7-dependent DCs express IL-1β and initiate the proliferation of FRCs (Benahmed et al., 2014). Both naïve and activated lymphocytes have a crucial role in FRC proliferation. DC-induced trapping of naïve lymphocytes in the lymph node can trigger the early proliferation of FRCs without inflammatory stimuli. The later phase of FRC proliferation is promoted by LTβR-expressing activated lymphocytes (Yang et al., 2014). The conduit network starts to shrink after the cell proliferation but remains enlarged compared to the naïve lymph node. This period is referred to as quiescence when the remodeled vascular-stroma is maintained. During quiescence, the FRCs are maintained in their remodeled form via the LTβR expressed by DCs. In addition to the DCs, the remodeled conduit network is also supported by B cells (Gregory et al., 2017; Kumar et al., 2015; Thierry et al., 2019). The lymph node is able to maintain its size exclusion into the parenchyma during early inflammation even though the conduit network is stretched and extracellular matrix components are reduced (Martinez et al., 2019).

LECs also undergo proliferation during inflammation, similarly to the other stromal populations. Soluble factors draining downstream into the lymph node or signals initiated within the lymph node can induce lymphangiogenesis (Angeli et al., 2006). The proliferation of both BECs and LECs is regulated by VEGF produced by several sources, including the reticular cells, DCs, and B cells, to accommodate the influx of lymphocytes and DCs (Thierry et al., 2019). When the pathogen is neutralized, the lymph node stroma will contract and return to homeostasis. The reduction of lymphoid and myeloid cells limits the trophic factors in the lymph node, which may lead to reduced proliferation of the stromal cells and increase their probability of apoptosis. Nevertheless, the cell number of the stromal cells is elevated after inflammation compared to the initial amount. After the first inflammation, the remodeling of the stroma is shorter and not as comprehensive in secondary inflammation. Even if the inflammation is resolved quickly, scarring is left in the tissue leading to damaged local immunity. The development of chronic inflammation

could also be a result of the scarring (Acton & Reis e Sousa, 2016; Thierry et al., 2019).

2.7 Animal models

2.7.1 CCL19-Cre x iDTR mouse model

The CCL19-Cre x iDTR (CCL19-iDTR) mouse model was generated by utilizing the Cre-loxP recombination system, which is used to modify a DNA sequence at a specific site in the DNA. The Cre recombinase recognizes the loxP sites and mediates the excision of the DNA sequence between the two loxP sites. CCL19-Cre mice (Chai et al., 2013) expressing the Cre recombinase under the *CCL19* promoter were bred with Cre-inducible diphtheria toxin receptor (iDTR) mice (Buch et al., 2005) expressing the diphtheria toxin receptor (DTR). The breeding resulted in mice expressing the DTR under the *CCL19* promoter in Cre+ animals (Figure 5).

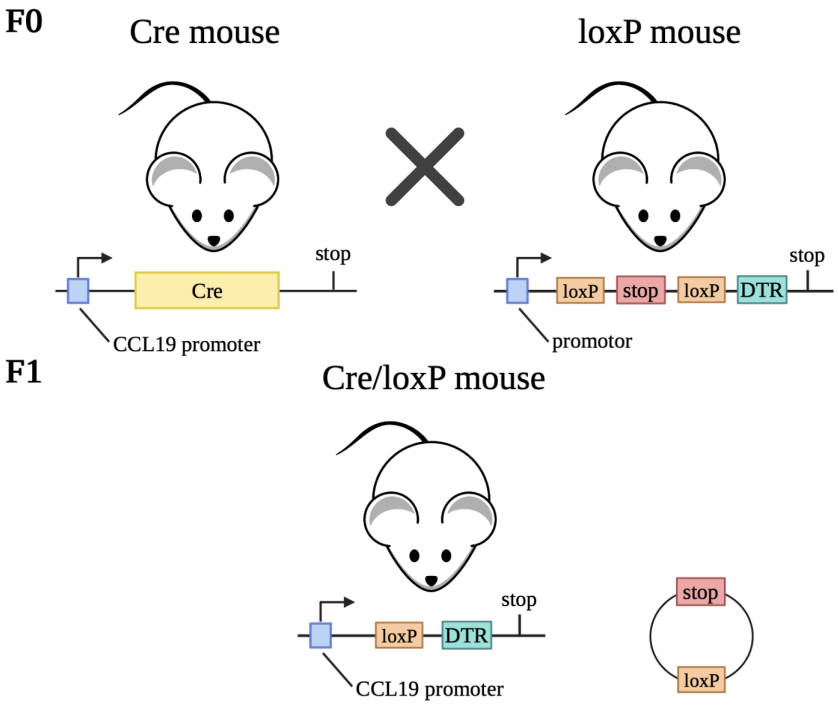

Figure 5. Schematic illustration of the Cre-loxP recombination system in CCL19-Cre x iDTR mice. In generation F0, the left mouse line expresses the Cre recombinase under the *CCL19* promoter, and the right mouse line has a stop cassette before the DTR, inhibiting the expression of DTR. By crossing the mouse lines, the stop cassette is removed and DTR is expressed in Cre+ mice. DTR is only expressed in CCL19+ cells and by injection of DT into the mouse, these specific cells go under apoptosis. Figure created with BioRender.

2.7.2 CCL19-Cre x tdTomato lox mouse model

The CCL19-Cre x tdTomato lox (CCL19-tdTomato) mouse model also utilizes the Cre-loxP recombination system. The CCL19-Cre mice (Chai et al., 2013) expressing the Cre recombinase under the *CCL19* promoter were bred with the reporter mice tdTomato lox. This resulted in mice expressing the red fluorescent tdTomato protein under the *CCL19* promoter in Cre+ animals (Figure 6).

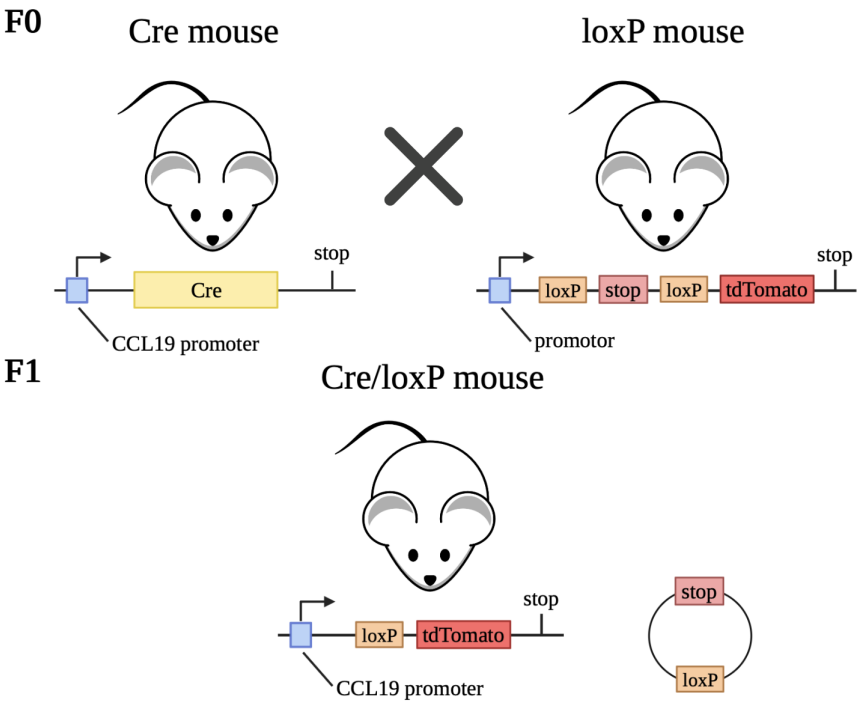

Figure 6. Schematic illustration of the Cre-loxP recombination system in CCL19-Cre x tdTomato lox mice. In generation F0, the left mouse line expresses the Cre recombinase under the *CCL19* promoter, and the right mouse line has a stop cassette before the protein tdTomato, inhibiting the expression of red fluorescent protein. By crossing the mouse lines, the stop cassette is removed and the red fluorescent protein is expressed in CCL19+ cells in Cre+ mice. Figure created with BioRender.

3 Aims of the study

Non-leukocytic stromal cells play key roles in regulating the immune responses. In the lymph nodes, FRCs produce cable-like matrix conduits, which allow instantaneous transfer of small soluble antigens into the parenchyma of the lymph node. Yet, the malleability of FRCs and conduits during the acute inflammatory expansion of the lymph nodes and their role in controlling the immune responses against different types of antigens during the immune response remain incompletely understood. This thesis was performed to clarify the role of the FRCs and the conduit in regulating the immune response in the lymph nodes. The aims of the thesis study are:

1. Establishing a local FRC depletion model in draining lymph nodes using the CCL19-Cre x iDRT mouse model

2. To study how the draining lymph node responds to inflammation when the FRC population is reduced

4 Materials and Methods

4.1 Animal models

Different mice models were used for the thesis. Mice were housed in the animal facility of the University of Turku. The mice were housed in individually ventilated cages with a light-dark cycle of 12 hours. The animals were *ad libitum* fed with chow pellets and water. All mice used were between the ages of 7 and 27 weeks. All animal experiments complied with the Ethical Committee for Animal Experimentation in Finland and were conducted according to the rules and regulations of the Finnish Act on Animal Experimentation (497/2013). The experiments took into consideration the principles of the 3Rs and were performed under the animal license number 14685/2020.

The wild-type strain C57BL/6NRj was purchased from Janvier Labs. The genetically altered mice, including the iDTR mice (C57BL/6-Gt(ROSA)26Sortm1(HBEGF)Awai/J), homozygous for the iDTR gene, and Tomato lox mice (B6.Cg-Gt(ROSA)26Sortm14(CAG-tdTomato)Hze/J), homozygous for tdTomato, were purchased from Jackson Laboratories. The CCL19-Cre mice have been described previously (Chai et al., 2013), and were bred with the iDTR mice and Tomato lox mice to create the mouse models used in the study. The breeding is described in 2.7 for both CCL19-iDTR and CCL19-tdTomato mice models. In experiments with the CCL19-iDTR mouse model, Cre- mice were used as a negative control since the DTR expression is not active in Cre- animals. The CCL19-tdTomato Cre- mice were used as a negative control in the validation of CCL19-expressing stromal cells in the lymph node, because the fluorescent protein is not expressed in Cre- mice.

4.2 Local FRC ablation *in vivo*

Multiple protocols with different timing and dosing of diphtheria toxin (DT, D0564 Sigma-Aldrich) were tested for local and systemic depletion of FRCs in both genders (Table 1) (protocol adapted from Cremasco et al., *Nat Immunol* 2014). The mice were anesthetized with isoflurane (1000 mg/g, Attane vet) before s.c. injecting 20 µl of DT diluted in commercial PBS into the hind leg footpads. The injection was performed with an insulin syringe with a 30G needle (324826, BD). The lymph nodes were harvested on day four or six for analysis with flow cytometry or imaging.

For the local ablation of the FRCs in the draining popliteal lymph node in female and male mice, DT with a concentration of 0.5 ng/g of body weight was s.c. injected one to three times (multiple injections on consecutive days) into one or both hind leg footpads (Table 1). The popliteal and axillary lymph nodes were harvested on day four or six. The

local depletion was also tested with DT with a concentration of 2 ng/g of body weight s.c. injected two times (multiple injections on consecutive days) into both hind leg footpads in female mice, and the popliteal and axillary lymph nodes were collected on day four or six.

The systemic depletion of the FRCs *in vivo* was tested in both male and female mice. The mice were given one 100 µl intraperitoneal (i.p.) injection of DT diluted in commercial PBS with a 30G needle (304000, BD). In female mice, the concentration of DT was 8 ng/g of body weight, whereas, in male mice, it was 5 ng/g of body weight. The popliteal and axillary lymph nodes were harvested on day four in females and on day six in males.

Table 1. The different FRC depletion protocols tested for local and systemic (i.p.) depletion of FRCs in CCL19-iDTR mice.

Concentration (ng/g)	No. of injection	Footpad	Time point	Gender
0.5 ng/g of body weight	1x	Left	Day 4	Female
0.5 ng/g of body weight	1x	Both	Day 4	Female
0.5 ng/g of body weight	3x	Left	Day 4	Female
2 ng/g of body weight	2x	Both	Day 4 & 6	Female
8 ng/g of body weight	1x	i.p.	Day 4	Female
0.5 ng/g of body weight	1x	Both	Day 4 & 6	Male
0.5 ng/g of body weight	3x	Both	Day 4 & 6	Male
5 ng/g of body weight	1x	i.p.	Day 6	Male

4.3 Inflammation model

On day four post-injection with DT, inflammation was induced by injecting a mixture of 18 µl Complete Freund's Adjuvant (CFA, F5881 Sigma-Aldrich) and 2 µl Ovalbumin antigen (1 mg/ml, vac-pova InvivoGen). The anesthetized mouse was s.c. injected with the mixture into the same hind leg footpad as the DT injection. The popliteal and axillary lymph nodes were harvested five days post-injection for imaging.

4.4 Flow cytometry

4.4.1 Preparing lymph node single-cell suspension

The popliteal and axillary lymph nodes were harvested from the mice, and single-cell suspensions were prepared from the lymph nodes. The lymph nodes were mechanically cut into smaller pieces and enzymatically digested. The samples were incubated two or

three times with an enzymatic cocktail containing 0.8 mg/ml Dispase (17105-041, Gibco), 0.2 mg/ml Collagenase P (11213865001, Roche), and 0.1 mg/ml DNase I (10104159001, Roche) in RPMI-1640 medium (R5886, Sigma-Aldrich). The tubes containing the tissues were incubated at +37 °C in a water bath and gently inverted every five minutes in the first round of digestion. After 20 min, the tissues were gently aspirated and expirated using a pipette, and large tissue fragments were allowed to settle for 30 s. Afterward, most of the supernatant was removed into 9 ml ice-cold FACS buffer (2% FCS + 5 mM EDTA in PBS), and 2-5 ml of enzyme cocktail was added to the tubes with the large tissue fragments for digestion. During the second round of digestion at room temperature, the contents were gently mixed with a pipette every 2-3 min for 10 min, followed by vigorously mixing for 30 s. Again, the tissue fragments were allowed to settle before removing the supernatant into the same tube with ice-cold FACS buffer as before, and 2-5 ml of enzyme cocktail was added to the tubes with the tissues. The third round of digestion was performed only by vigorously mixing the cells every 5 min with a pipette until all remaining tissue fragments had been digested. All supernatant was collected into the ice-cold FACS buffer, and the cells were pelleted by centrifugation at +4 °C/300 g/4 min, followed by collecting the cells in the supernatant, washing the cells with EPICS I (PBS + 2% FCS + 0.01% NaN_3), and filtering through 77 µm silk to remove cell aggregates.

4.4.2 Fluorescence-activated cell sorting

After obtaining the single-cell suspensions, the samples were transferred to a 96-well plate with a U bottom. The cells were stained with the viability marker Fixable Viability dye-eFluor 450 (65-0863, eBioscience) 1:1000 in PBS for 15-30 min to exclude dead cells. The samples were washed twice with EPICS I and centrifuged at +4-8 °C/2000 rpm/3 min. Unspecific staining of antibodies to endogenous Fc receptors was blocked with anti-CD15/CD32 mouse Fc block (BE0307, BioXCell) 1:100 in EPICS I for 10 min. The samples were then stained with fluorescently conjugated antibodies (Table 2), incubated for 20-30 min on ice, washed twice with EPICS I, and centrifuged at +4-8 °C/2000 rpm/3 min, and, if needed, fixed using EPICS FIX (PBS + formaldehyde). All samples were acquired with the cytometer LSR Fortessa and analyzed using FlowJo software, both from BD.

Table 2. Antibodies against mouse antigens used in flow cytometry.

Antibody	Clone	Cat. No.	Company	Conc.
B220-AF647	RA3-6B2	103226	BioLegend	1:200
B220-BV421	RA3-6B2	562922	BD	1:200
CD3-AF647	17A2	557869	BD	1:200
CD3-PE	17A2	555275	BD	1:200
CD31-AF488	MEC13.3	102514	BioLegend	1:200
CD31-BV711	390	102449	BioLegend	1:200
CD45-APC	30-F11	557659	BD	1:200
CD45-PerCP Cy5.5	30-F11	550994	BD	1:200
PDPN-APC	8.1.1	127410	BioLegend	1:200
PDPN-PE Cy7	8.1.1	127412	BioLegend	1:200
Ter119-BV785	Ter119	116245	BioLegend	1:200
Ter119-PE/Dazzle594	Ter119	116244	BioLegend	1:200

4.5 Microscopy

The popliteal, inguinal, and axillary lymph nodes were collected from the CCL19-iDTR mice and embedded in optimal cutting temperature (OCT) medium. From the CCL19-tdTomato mice, the popliteal, inguinal, and axillary lymph nodes were collected and fixed with 4% paraformaldehyde for 2 hours at room temperature followed by 2 hours at +4 °C, then washed with PBS twice for 10 min and incubated in 30% sucrose overnight at +4 °C. The lymph nodes were embedded in OCT in a predetermined orientation. The tissue blocks were snap frozen using dry ice and stored at -70 °C. Lymph nodes were cut in 6 µm transverse sections with the cryotome. The tissue sections were stained with fluorescently conjugated antibodies, or primary antibodies followed by conjugated secondary antibodies at room temperature (Table 3). The sections were overlaid with ProLong Gold Antifade Mountant without DAPI (P36930, Invitrogen).

Fluorescence images were imaged using the LSM880 confocal microscope (Carl Zeiss) with Plan-Apochromat 20x/0.8 objective by taking tile scans. The images were acquired with the Zen 2.3 SP1 software (Carl Zeiss).

Image analyses were performed with ImageJ software (NIH). For all images, the background was subtracted, and the brightness and contrast were adjusted linearly. Staining controls were performed for the secondary antibodies, and the Cre- tissues were used as controls for the Cre+ tissues in all stainings. All controls were treated the same way as the samples.

Table 3. Antibodies against mouse antigens used in microscopy.

Antibody	Clone	Cat. No.	Company	Conc.
B220-AF647	RA3-6B2	103226	BioLegend	10 µg/ml
CD3-AF647	17A2	557869	BD	10 µg/ml
CD11b-AF488	M1/70	101217	BioLegend	5 µg/ml
CD31-AF488	MEC13.3	102514	BioLegend	10 µg/ml
CD31-AF647	390	102416	BioLegend	10 µg/ml
CD169	3D6.112	MCA884EL	AbD Serotec	5 µg/ml
Collagen I	pAb	AB765P	Millipore	10 µg/ml
Collagen IV-AF488	pAb	1340-01	Southern Biotech	1:100
ER-TR7-DyL405	ER-TR7	NB100-64932V	Novus Biologicals	5 µg/ml
Fibronectin	pAb	F3648	Sigma-Aldrich	1:400
LYVE1-eFluor660	ALY7	50-0443-90	Invitrogen	5 µg/ml
Podoplanin	8.1.1	8.1.1	DSHB	1:50
TER119-AF488	TER-119	116215	BioLegend	10 µg/ml
Donkey anti-goat IgG AF488	pAb	A11055	Invitrogen	5 µg/ml
Goat anti-hamster IgG AF546	pAb	A21111	Invitrogen	5 µg/ml
Goat anti-mouse CD31	pAb	AF3628-SP	R&D	10 µg/ml
Goat anti-rabbit IgG AF564	pAb	A11035	Invitrogen	5 µg/ml

4.6 Statistical analysis

For comparing results from two different groups, the data was analyzed using Mann-Whitney U test. The numerical data is presented as mean $\pm$ SD. The statistical analyses were conducted with GraphPad Prism software, and a P-value under 0.05 was considered as statistically significant.

5 Results

5.1 CCL19-tdTomato is mostly expressed in the FRCs

The CCL19-tdTomato mouse is a reporter mouse that expresses the tdTomato fluorescent protein in CCL19-expressing cells. To verify the CCL19-tdTomato reporter mouse, lymph nodes were harvested from CCL19-tdTomato mice and used for FACS and imaging to examine how many percent of the stromal cells express the fluorescent reporter (tdTomato) and where it is expressed in the lymph node. The histograms confirm that the FRCs (64.8%) and LECs (28.6%) express the tdTomato protein under the CCL19 promotor in Cre+ mice (Figure 7a). Cre- mice are used as a negative control in the histograms since the mice do not express the fluorescent reporter. BECs did not express tdTomato and are therefore $CCL19^{-}$. The CCL19-tdTomato positive cells can be seen in the T cell zone and interfollicular region where the FRCs reside in the popliteal lymph node (Figure 7b). Furthermore, the zoom-in shows how the CCL19-tdTomato is expressed on the $CD31^{+}$ lymphatic endothelial cells (arrowhead) and FRCs (arrow).

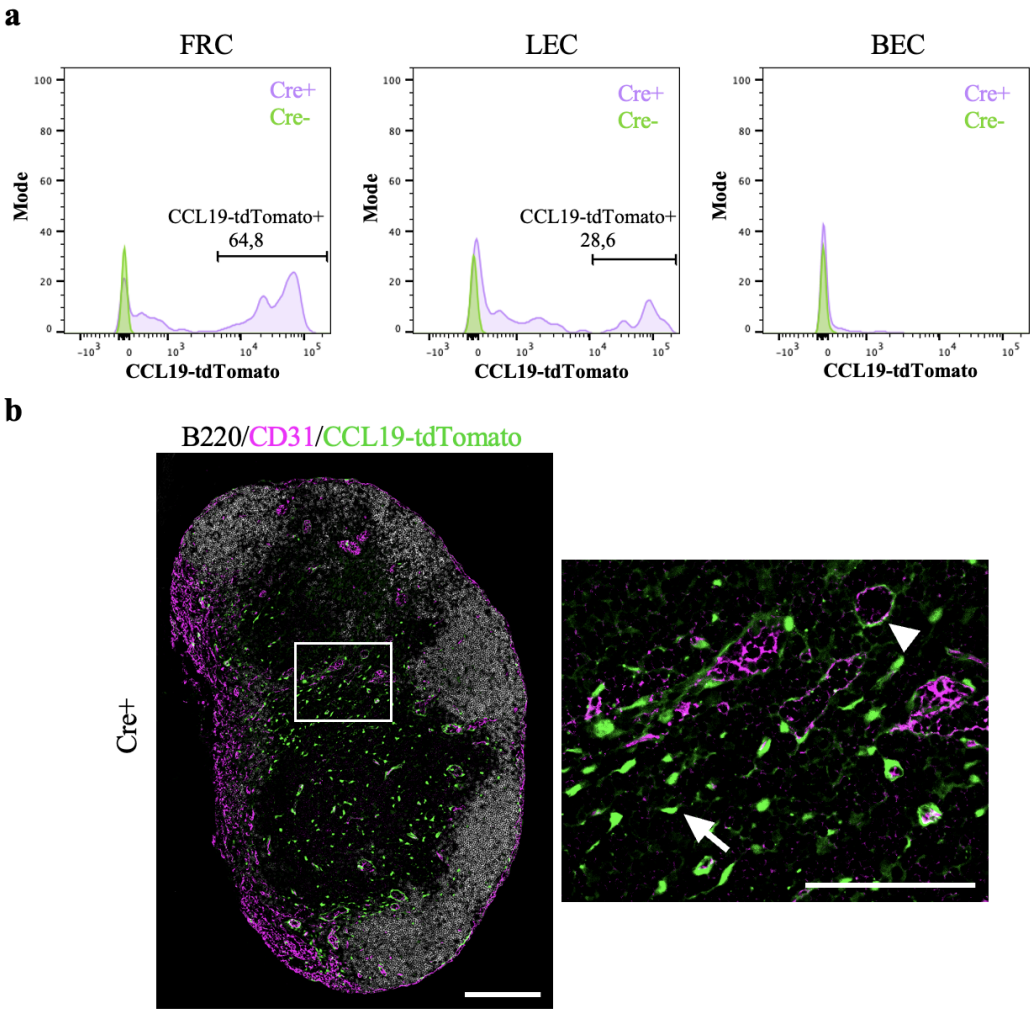

Figure 7. CCL19-tdTomato expression in lymph node stromal cells. **a**, Representative histograms of protein expression for CCL19-tdTomato in stromal cells isolated from CCL19-tdTomato mice lymph nodes. The bars indicating the positive peaks for expression of CCL19-tdTomato were determined based on Cre- mice. **b**, Representative tile scan of B220^{+} (B cells, grey), CD31^{+} (endothelial cells, magenta), and CCL19-tdTomato^{+} (CCL19+ cells, green) cells in CCL19-tdTomato Cre+ lymph node. Arrowhead indicates CCL19-tdTomato+ CD31^{+} endothelial cells, arrow indicates CCL19-tdTomato+ FRCs. Scale bar, 200 µm (zoom-in T cell area (white box), 100 µm).

5.2 Expression of Cre or iDTR does not effect FRC count

To make sure that the Cre or iDTR does not affect the FRC number, we needed to assess the initial amount of stromal cells in naïve untouched lymph nodes. If either Cre or iDTR affects the FRC number, then we would need to take it into account when assessing the depletion. The number of stromal cells was assessed in female CCL19-iDTR mice and female C57BL/6N wild-type mice to see if the CCL19-Cre affects the stromal cell populations. The weights of the popliteal (Figure 8a) and axillary (Figure 8b) lymph nodes were compared between the mouse strains. The quantification shows that there is no significant difference between the weights of the popliteal or the axillary lymph nodes in the different mice strains.

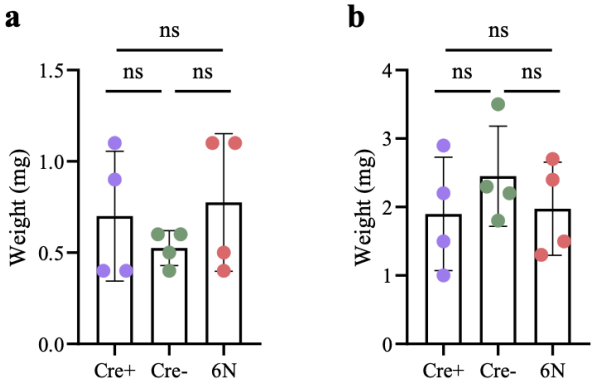

Figure 8. Tissue weights of naïve popliteal and axillary lymph nodes from Cre+ and Cre- CCL19-iDTR mice and C57BL/6N wild-type mice. Quantification of popliteal (**a**) and axillary (**b**) lymph node weights. Data are represented as mean ±SD error bars, Mann-Whitney *U* test (two-tailed), ns, not significant. N=4 lymph nodes from two independent experiments.

The harvested lymph nodes were enzymatically digested into single-cell suspension samples. The samples were analyzed with FACS to study the cell numbers in the lymph nodes between the different strains (Figure 9a,c,e,g) (gating strategy; Appendix A). The quantification of the FRCs in the popliteal lymph node (Figure 9b) shows that both the percentage and cell number are slightly higher in one of the C57BL/6N wild-type mice compared to the Cre+ and Cre- CCL19-iDTR mice, but the popliteal lymph nodes are overall comparable between the strains. The two different mouse strains are also comparable in the axillary lymph nodes in the percentage and cell number of the FRCs (Figure 9d). Even though there is a marginal difference between the strains in the FRC population, the Cre+ and Cre- mice have a similar initial amount of FRC. We were also interested in the B cell population since it has been previously shown that the FRCs support the B cells (Cremasco et al., 2014), and we wanted to see if the depletion model has an effect on the

B cells. In all the naïve lymph nodes, the percentage of the B cells and cell numbers were similar between the strains (Figure 9f,h).

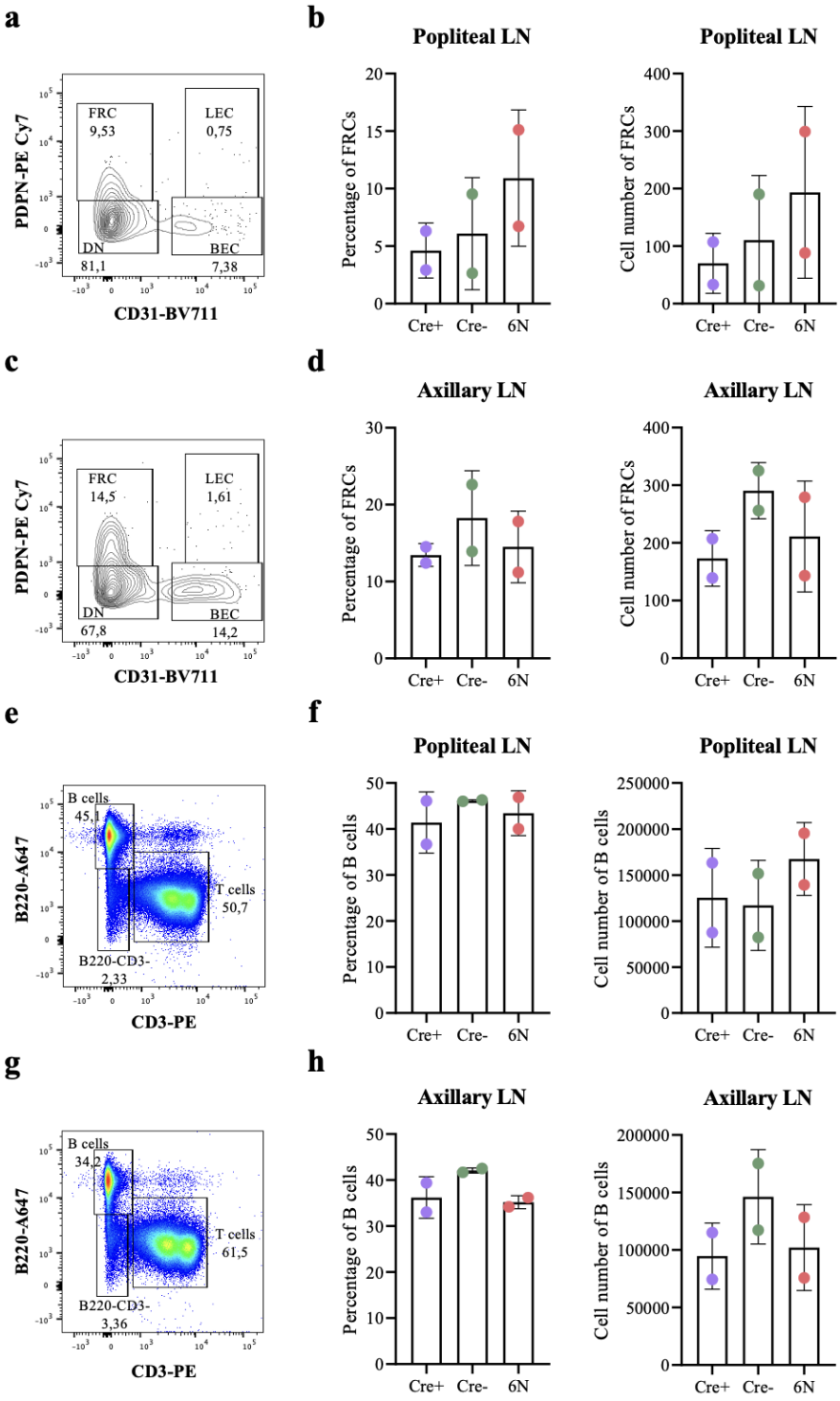

Figure 9. Comparison of the percentage and cell number of FRCs and B cells in popliteal and axillary lymph nodes. Representative FACS contour plots of the stromal cells in popliteal (**a**) and axillary (**c**) lymph nodes. FRC percentage and cell number in popliteal (**b**) and axillary (**d**) lymph nodes. Representative FACS dot plots of the lymphocytes in popliteal (**e**) and axillary (**g**) lymph nodes. Percentage and cell number of B cells in popliteal (**f**) and axillary (**h**) lymph nodes. Error bars indicate SD, each data point represents two lymph nodes combined from two independent experiments. Lymph node (LN).

5.3 Local *in vivo* depletion reduces the FRC population in the draining lymph node

The first aim of the thesis was to establish a local FRC depletion model in the draining lymph nodes of CCL19-iDTR mice. To achieve this aim, DT with a concentration of 0.5 ng/g of weight was s.c. injected once into one hind leg footpad into female Cre+ and Cre- mice on day one, and the popliteal and axillary lymph nodes were harvested on day four (Figure 10a). The weights of the Cre+ and Cre- draining and non-draining popliteal lymph nodes were compared to each other (Figure 10b). The axillary lymph nodes' weights were compared in the same way as the popliteal lymph nodes. There was a significant difference in the weights between the Cre+ and Cre- draining popliteal lymph nodes. About 50% of the Cre+ popliteal lymph node weight has been reduced compared to the Cre- popliteal, where no depletion occurs. The axillary lymph nodes on the draining side in the Cre+ and Cre- mice are also similar in size, supporting that the reduction in the total cell number only occurs in the popliteal lymph nodes. Comparing the weights of the Cre+ and Cre- non-draining popliteal and axillary lymph nodes, there was no significant difference between the weights. This suggests that the non-draining side is not affected by the DT injection.

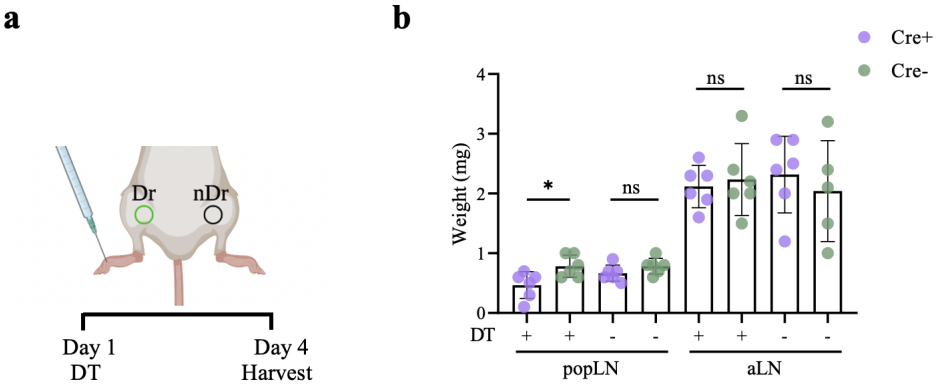

Figure 10. Tissue weights of popliteal and axillary lymph nodes after FRC depletion. **a**, Schematic illustration of the depletion strategy with DT in CCL19-iDTR mice. **b**, Quantification of popliteal and axillary lymph node weights in DT *in vivo* depleted lymph nodes. Data are represented as mean ±SD error bars, Mann-Whitney *U* test (two-tailed), *P<0.05, ns, not significant. n indicates lymph nodes (n=5-6) over three independent experiments. Draining popliteal lymph node (Dr), non-draining popliteal lymph node (nDr).

The harvested lymph nodes were used for FACS to analyze the FRC population from the different stromal cell populations (Figure 11a,d). The percentage (Figure 11b,e) and cell number (Figure 11c,f) of the FRCs from the Cre+ and Cre- draining and non-draining popliteal and axillary lymph nodes were quantified. In the Cre+ draining popliteal lymph node, the percentage and the cell number of the FRCs have both been reduced by about 50% compared to the other lymph nodes. Thus, the depletion of the FRCs has, in this model, approximately a 50% success rate in the draining popliteal lymph node. By looking at the percentage of the FRCs in the Cre+ draining axillary lymph node, the percentage is comparable to the other axillary lymph nodes. However, the cell number is lower in the Cre+ draining axillary than in the other axillary lymph nodes. This indicates that there is some FRC depletion in the Cre+ draining axillary lymph node, and the FRC depletion is not local. In both the popliteal and axillary lymph nodes, percentage and cell number are similar between the Cre- lymph nodes and the non-draining Cre+ lymph node.

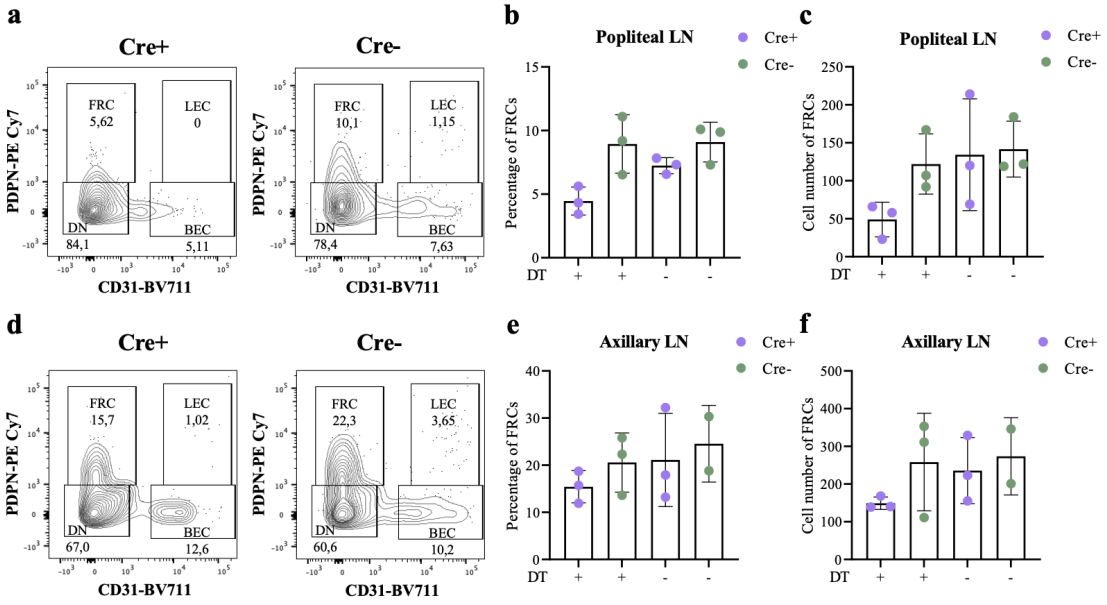

Figure 11. Assessment of local *in vivo* depletion model. Representative FACS contour plots comparing Cre+ and Cre- stromal cell subpopulations in the popliteal (**a**) and axillary (**d**) lymph nodes. FRC percentage and cell number of draining and non-draining popliteal (**b,c**) and axillary (**e,f**) lymph nodes. Data are represented as mean ±SD error bars from three independent experiments with each data point representing two lymph nodes combined. Lymph node (LN).

Because the FRC population supports the B cell population in the lymph node (Cremasco et al., 2014), the B cells were quantified in the Cre+ and Cre- draining and non-draining popliteal and axillary lymph nodes to assess if the B cells have been affected by the depletion (Figure 12a,d). The DT-draining Cre+ popliteal lymph node has a reduced B cell percentage compared to the other lymph nodes (Figure 12b). The percentage of the B cells in the Cre+ non-draining, Cre- draining, and non-draining popliteal lymph nodes are in line with the FRC reduction in the corresponding popliteal lymph nodes in Figure 11b. Nevertheless, the cell number is reduced in both the Cre+ popliteal lymph nodes, regardless of the injection side (Figure 12c). In the axillary lymph nodes, the percentage (Figure 12e) and cell number (Figure 12f) of the B cells are reduced in the Cre+ draining lymph nodes. These results are similar to the results in Figure 11, supporting that the depletion is not local.

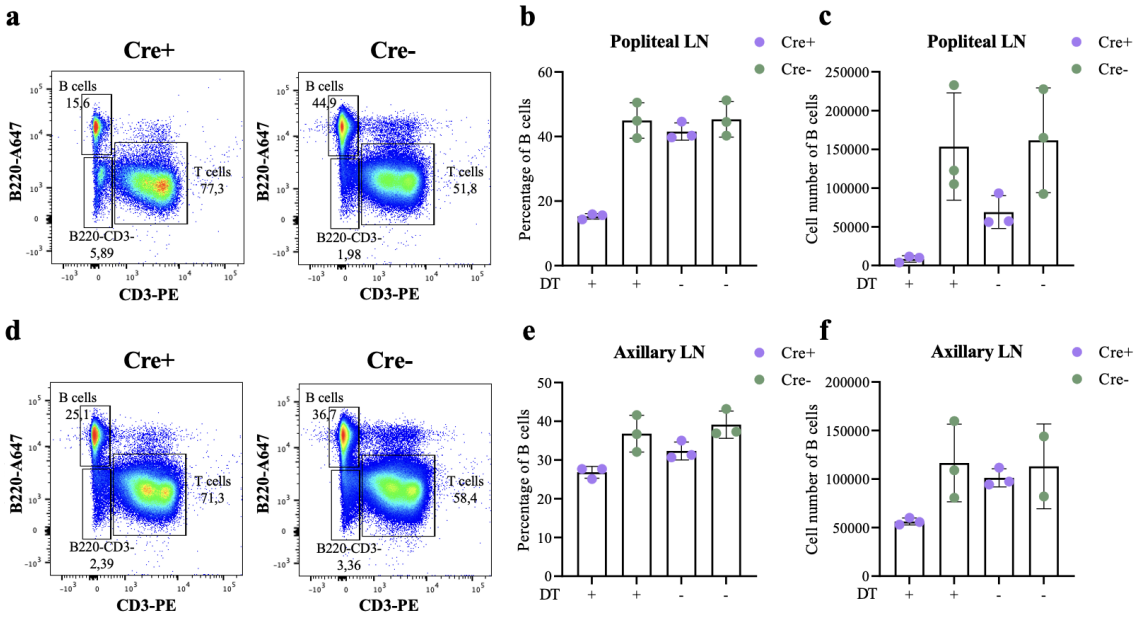

Figure 12. *In vivo* depletion of CCL19^{+} FRCs reduces the amount of lymph node B cells in both Cre+ draining and non-draining lymph nodes. Representative FACS dot plots comparing Cre+ and Cre- B cells in the draining and non-draining popliteal (**a**) and axillary (**d**) lymph nodes. Percentage and cell number of B cells in draining and non-draining popliteal (**b,c**) and axillary (**e,f**) lymph nodes. Each point represents two lymph nodes combined with error bars indicating mean ±SD from three independent experiments. Lymph node (LN).

Confocal imaging was used to study the morphological changes in the FRC-depleted lymph nodes. Both popliteal lymph nodes from the CCL19-iDTR mice were used for microscopy, where the DT-draining popliteal lymph node was compared to the non-draining popliteal lymph node (negative control). To study the morphology of the lymph nodes in Cre+ and Cre- draining and non-draining popliteal lymph nodes, frozen lymph node sections were stained with Collagen type I (Col I), which is a marker for the collagen core of the conduit. The Cre+ draining popliteal (Figure 13a) has a denser amount of Col I compared to the Cre+ non-draining (Figure 13c) and Cre- draining popliteal (Figure 13b) lymph nodes, and the whole lymph node has a compressed appearance, losing the B cell follicles and T cell area. In the Cre+ non-draining and Cre- draining popliteal lymph nodes, the presence of Col I is normal, and the lymph node morphology is typical with defined structures, e.g., medullary sinus and B cell follicles. The Cre+ non-draining and Cre- draining popliteal lymph nodes are also similar in size, correlating with the quantified lymph node weights (Figure 10b).

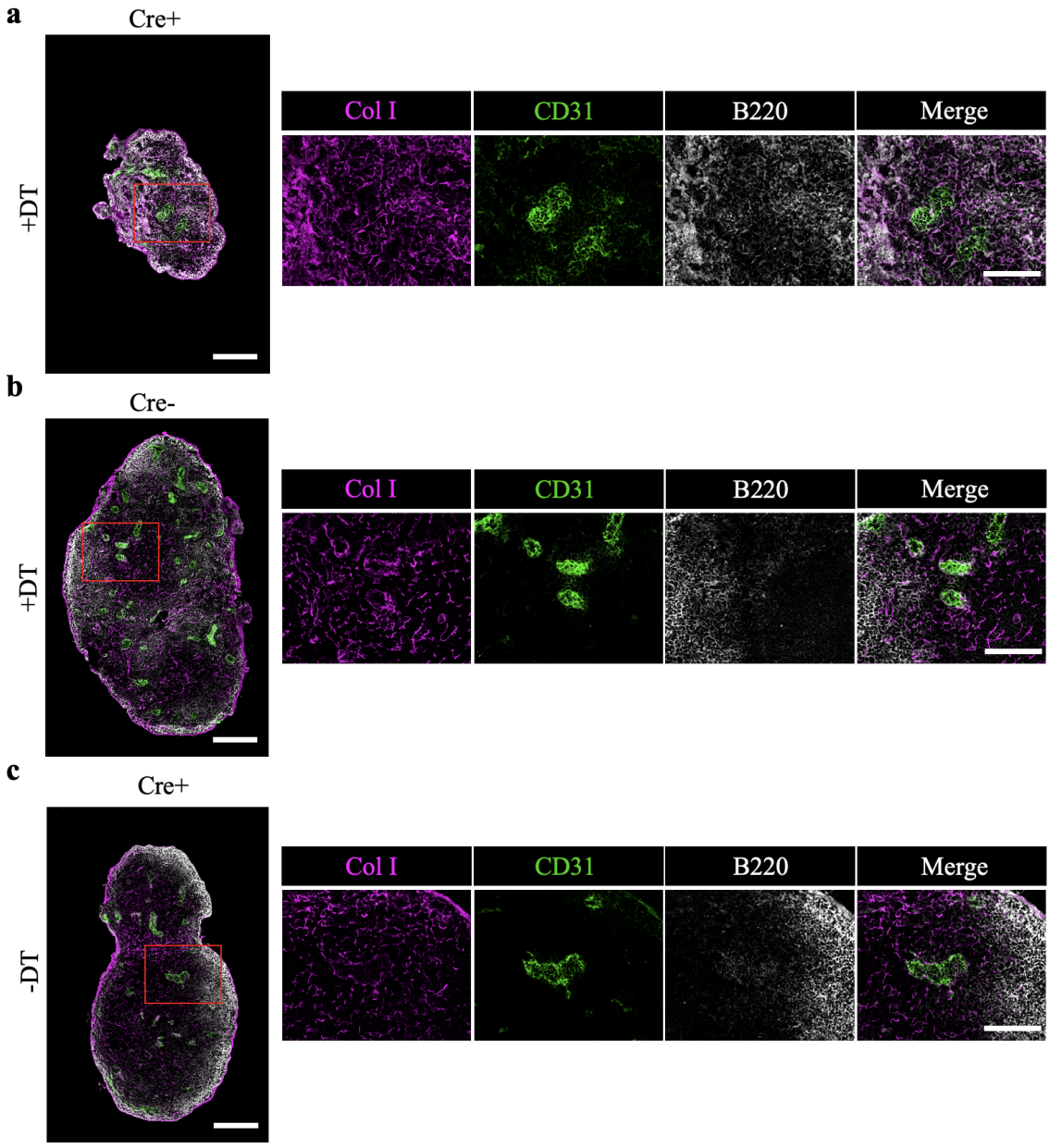

Figure 13. The Cre+ draining popliteal lymph node shrinks during FRC-depletion, and loses its defined compartments. Representative images of lymph node frozen section stained for Col I (conduit core, magenta), CD31 (endothelial cells, green), and B220 (B cells, grey) in Cre+ draining popliteal (**a**), Cre- draining popliteal (**b**), and Cre+ non-draining popliteal (**c**) lymph nodes. Scale bars, 200 μm (zoom-in T cell area (red box), 100 μm).

5.4 The draining lymph node can expand after FRC depletion

The second aim of the thesis was to study how the draining lymph node responds to inflammation when the FRC population is depleted. The FRCs were depleted *in vivo* by injecting DT (0.5 ng/g of body weight), and then inflammation was induced on day four by injecting a mixture of CFA and Ovalbumin into the footpad. The popliteal and axillay lymph nodes were harvested on day five of inflammation when an acute inflammation has been induced in the draining lymph node (Figure 14a). The weights of the inflamed draining and non-draining popliteal lymph nodes were compared to the FRC-depleted popliteal lymph nodes (Figure 14b). The comparison shows that the Cre- draining popliteal lymph node injected with DT + CFA is able to induce an inflammatory response based on the expansion of the lymph node, but the Cre+ draining popliteal lymph node injected with DT + CFA is not able to expand as normal during inflammation when the FRCs are reduced. The weights of the inflamed Cre+ draining popliteal lymph nodes have only doubled in size compared to the Cre+ FRC-depleted popliteal lymph nodes, whereas the inflamed Cre- draining popliteal lymph nodes have increased 8-fold in their weight compared to the Cre- FRC-depleted popliteal lymph nodes.

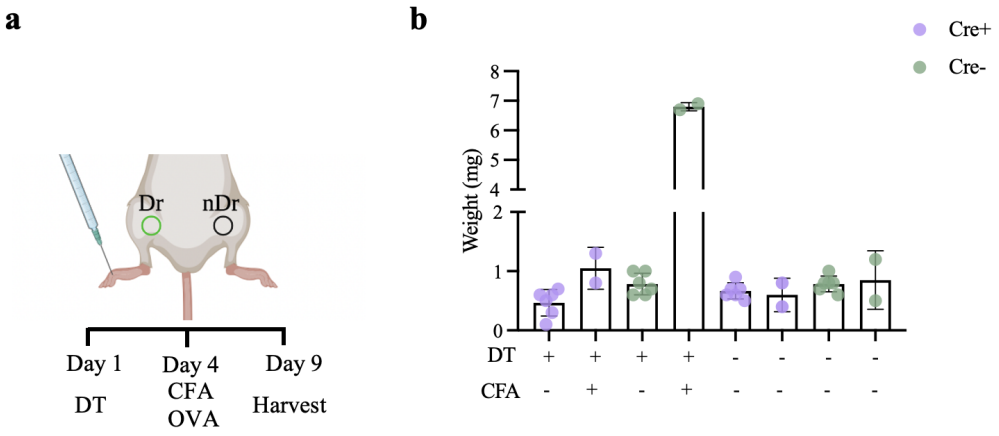

Figure 14. Lymph node expansion during inflammation after FRC depletion. **a**, Schematic illustration of the DT and immunization strategy for CCL19-iDTR mice. **b**, Quantification of popliteal lymph node weights in FRC-depleted lymph nodes and inflamed lymph nodes. Data are represented as mean ±SD error bars, and n indicates lymph nodes (n=2-6) over four independent experiments. Complete Freund's Adjuvant (CFA), diphtheria toxin (DT), draining popliteal lymph node (Dr), non-draining popliteal lymph node (nDr), and Ovalbumin (OVA).

Confocal imaging was also used for the inflammation model in the FRC-depleted lymph nodes to investigate their morphology. We used the popliteal lymph nodes from both sides in Cre+ and Cre- mice, and the non-draining lymph nodes were used as negative controls. The frozen lymph node sections were stained with the same antibodies as the FRC-depleted lymph nodes, making them comparable to each other. An immune response is indicated to be ongoing in the inflamed Cre+ FRC-depleted popliteal lymph node since the lymph node has expanded, and the presence of Col I seems to be denser than normal inflammation (Figure 15a). The inflamed Cre+ FRC-depleted popliteal lymph node has a more characteristic morphology with defined compartments than the Cre+ FRC-depleted popliteal lymph node in Figure 13a, but the morphology is not entirely normal. The inflamed Cre- draining popliteal lymph node has induced inflammatory expansion normally, thus the whole lymph node has increased in size and the B cell follicles have enlarged to help with the inflammation (Figure 15b). The Cre+ non-draining popliteal lymph node (Figure 15c) has a typical morphology with defined compartments similar to the Cre+ non-draining and Cre- draining lymph nodes in Figure 13 since all of them are theoretically non-treated popliteal lymph nodes.

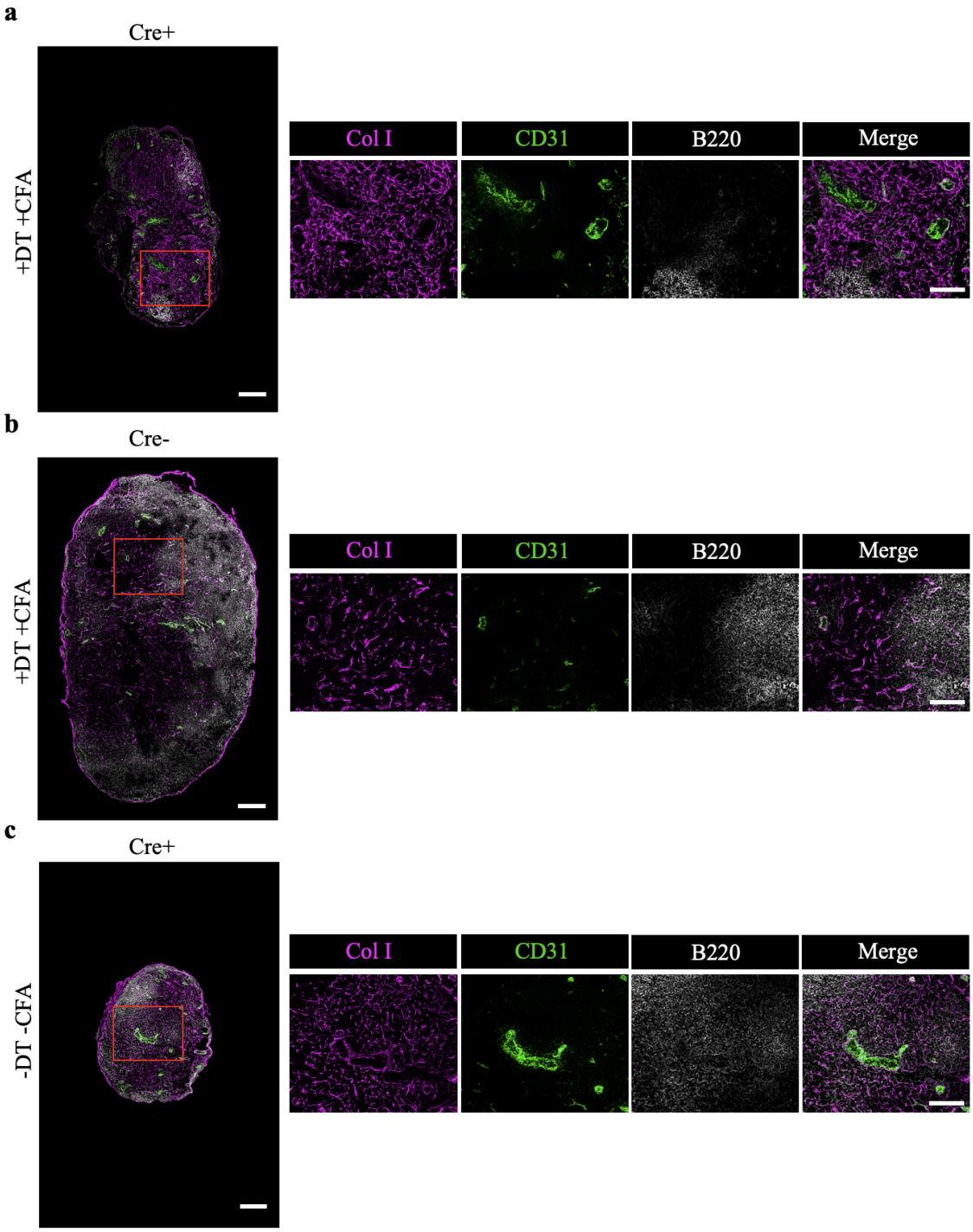

Figure 15. The draining popliteal lymph node responds to immunization after FRC depletion. Representative images of lymph node frozen section stained for Col I (conduit core, magenta), CD31 (endothelial cells, green), and B220 (B cells, grey) in Cre+ popliteal lymph node injected with DT and CFA (**a**), Cre- popliteal lymph node injected with DT and CFA (**b**), and Cre+ non-draining popliteal lymph (**c**). Scale bars, 200 μm (zoom-in T cell area (red box), 100 μm).

6 Discussion

6.1 CCL19$^+$ cells express CCL19-tdTomato

The main aim of the thesis was to study how the reduction of FRCs affects the draining lymph node during inflammation. FRCs are commonly known to be CCL19$^+$ (Luther et al., 2000), and a reporter mouse expressing the tdTomato fluorescent protein in CCL19$^+$ cells has been generated. The reporter mouse has been generated from CCL19-Cre mice bred with tdTomato lox mice. The expression of CCL19$^+$ cells needed to be verified to see whether the model was working for us and to be able to repeat published results. The CCL19-tdTomato mouse model was also used for visualizing which cells express CCL19 in the CCL19-iDTR strain. Both the FRCs and LECs expressed CCL19-tdTomato in Cre+ mice (Figure 7a), but the percentage of CCL19$^+$ cells is lower in the FRCs and higher in the LECs than it has been previously reported, 80-90% in FRCs and $<$10% in LECs (Chai et al., 2013). The image and the zoom-in reveal that some LECs express the fluorescent protein, but the majority do not express the CCL19-tdTomato protein, which correlates with the result from the FACS (Figure 7b). The CCL19-tdTomato fluorescent protein is expressed in the T cell zone, which supports that the excision of one of the loxP sites has been successful since the majority of the FRCs reside there. One explanation for the difference in the FRCs could be that Cre affects the expression of CCL19-tdTomato. The activity of Cre can be mosaic, where the Cre recombinase is not active in every cell, resulting in incomplete recombination in the cells. Since the stromal cells constitute only a couple percentages of the total cells in the lymph node, inconsistent expression of CCL19-tdTomato has a bigger effect in a small cell population than a large population. Chai et al. (2013) digested the tissues using a different protocol than ours, and they also enriched the stromal cell fraction, which usually causes more loss of cells but increases the frequency of the stromal cells. If we also had enriched the stroma cells, the percentage and cell number of the stroma would have increased, and the results could have been more similar. The variation can also depend on the parent-of-origin of the Cre recombinase. It has been shown that the variation in Cre activity could be due to whether the Cre transgene is inherited from the maternal or paternal side (Hayashi et al., 2003; Heffner et al., 2012). In our breeding, Cre comes from the paternal side because Cre seems to be inherited better from the paternal side.

6.2 FRC cell number is not affected by the transgenes

The initial amount of FRCs was similar between the Cre+ and Cre- CCL19-iDTR mice and C56BL/6N wild-type mice. To know how effective the depletion of the FRCs was *in vivo*, the initial amount of FRCs needed to be assessed in both female CCL19-iDTR and C57BL/6N wild-type mice to see if they had the same starting point and that Cre or iDTR does not effect the FRC numbers. The percentage and cell number of the FRCs were slightly lower in the popliteal lymph node in Cre+ and Cre- CCL19-iDTR mice compared to one of the the wild-type mice (Figure 9b). Even though there was no significant difference between the weights of the naïve popliteal and axillary lymph nodes between the strains (Figure 8), two of the popliteal lymph nodes in the Cre+ CCL19-iDTR and C57BL/6N wild-type mice had about double the weight compared to the other two popliteal lymph nodes in the groups (Figure 8a). Lymph nodes with higher weights have higher cell count, which could increase the FRC population cell number and percentage. Larger lymph node weight could also indicate an increase in the number of lymphocytes and no increase in the FRC cell number. The cell number composition of lymph nodes with higher weights can differ quite much compared to lymph nodes with lower weights. The natural difference between individual animals can affect the results. By increasing the number of experiments done, the natural difference will even out, which would have helped with the variation between the popliteal lymph nodes in Figure 9b. Another explanation for the difference between the data points in the different strains could be the isolation of the cells. We noticed that the stromal cells are hard to isolate, and we could see a clear difference if the tissues were digested two or three rounds with the enzymatic cocktail. Depletion of $CD45^+$ lymphocytes and $Ter119^+$ red blood cells would have enriched the stromal cells, but then the B cells would have been lost. FRCs have been shown to support the B cell survival, thus the initial amount was evaluated to see if they differed between the strains (Cremasco et al., 2014). There were no differences between the strains in either the B cell number or percentage in the popliteal or axillary lymph node at the starting point (Figure 9f,h).

6.3 *In vivo* depletion of FRCs

Establishing a local FRC depletion model in the draining lymph nodes of CCL19-iDTR mice was the first aim of the thesis. DT is widely used for different ablation models to study the function of the target cells *in vivo*. Specific genetic models targeting the FRCs have not been available before the CCL19-Cre mice were generated. Thus, the generation of the CCL19-iDTR mouse line was the first mouse model that could manipulate the

FRCs *in vivo* (Cremasco et al., 2014). Multiple protocols with different dosing of DT and timing were tested to find the optimal protocol to achieve a local depletion. We decided to use female mice because the male mice had inconsistent depletion efficiency. Sometimes, the depletion was effective, and other times, no depletion happened, which made the results not reproducible. With female mice, the depletion had repeatedly similar efficiency, and the results were reproducible. The depletion was systemic when injecting 2 ng/g of body weight of DT s.c. into the mice hind leg footpad since the FRCs were reduced in all Cre+ lymph nodes compared to the Cre- lymph nodes. It has previously been shown that the FRC network is notably damaged during 2 ng/g of body weight i.p. injection of DT, reducing the FRC cell number by 70%. In silico topological models predict that the FRC network robustness will significantly decrease when the FRCs are depleted $>$ 50%, and the lymph node can only tolerate a 50% loss of the FRCs in total (Novkovic et al., 2016). Cremasco et al. (2014) used a concentration of 0.5 ng per gram of body weight of DT for the local depletion, and we decided to use the same concentration after acquiring the results from the injections with 2 ng/g of body weight of DT. The number of injections and whether the injection should be in one or both hind leg footpads were also evaluated. Mice injected with DT on three consecutive days at 24-hour intervals into one footpad underwent depletion in both the draining and non-draining popliteal lymph nodes. By only injecting DT once into one hind leg footpad, we could compare the draining and non-draining lymph nodes against each other and evaluate if the depletion was local. In addition to local depletion, systemic depletion of the FRCs was also tested by injecting DT i.p. once into both genders. In male mice, the depletion was systemic, and the FRC population was reduced by over 50%. Due to the inconsistency in the local depletion in male mice, no further experiments were conducted. When testing systemic depletion in female mice, the depletion was less effective than the local depletion. The concentration of the DT was higher in the systemic depletion, but since the injection was i.p., the toxin is spread around the whole body compared to the local depletion where the toxin is concentrated in the draining lymph node. We decided not to proceed with the systemic depletion in female mice since it was thought to be used as a control for the local depletion.

6.4 Single injection of DT reduces the FRC population

Comparison of the weights between the Cre+ and Cre- lymph nodes will indicate if a change in the lymphocyte population has occurred due to the changes in the FRCs. The changes in the weights are not a direct effect due to the FRC depletion but a secondary effect from the change in the lymphocyte compartment. There was a significant difference

between the weights of the Cre+ and Cre- draining popliteal lymph nodes, whereas there was no significant difference between the Cre+ and Cre- non-draining popliteal, draining, and non-draining axillary lymph nodes (Figure 14). The weight of the Cre+ draining popliteal lymph nodes has reduced by about 50% compared to the Cre- draining popliteal lymph nodes. A comparison of the lymph node weights suggests that the depletion is local, but the data from the FACS indicates that the FRC depletion is not local (Figure 11, 12). The tissue weights only tell us about the changes in the total cell number, especially the lymphocyte number, but nothing about the stromal cells since they are such a small percentage of the total cells. However, the different cell populations are analyzed with FACS and show if the depletion is local or not. To estimate if the depletion is local, both the popliteal and axillary lymph nodes are examined. The popliteal lymph node is the first draining lymph node from the hind leg footpad, and the axillary lymph node is on another draining chain and drains seldom from the footpad (Harrell et al., 2008). If the FRC population is changed in the axillary lymph node, then it indicates that the depletion is systemic and not local. The depletion is systemic due to the DT having drained into the axillary lymph node either from the footpad injection via the inguinal lymph node or circulating through the body. The quantification of the popliteal lymph nodes from the FACS shows that both the percentage and cell number of the FRCs were reduced in the Cre+ draining lymph node in contrast to the Cre- popliteal and Cre+ non-draining popliteal lymph nodes (Figure 11b,c). The FRCs have decreased about 50% in the Cre+ draining popliteal lymph node compared to the other lymph nodes. Novkovic et al. (2016) showed that i.p. injection of 0.5 ng/g of body weight DT resulted in moderate FRC depletion, and the FRC number was reduced by 37% in the inguinal lymph nodes. These results are in the same direction since i.p. injection spreads to a bigger area than s.c. injection and the toxin is not focusing on a single draining path. In the axillary lymph nodes, the FRC percentage and cell number are also slightly reduced in the Cre+ draining lymph node (Figure 11e,f). The results of the B cells reinforce the indication that the depletion is not local (Figure 12). The percentage and cell number of the B cells are reduced in both the Cre+ draining popliteal and axillary lymph nodes. The reduction of FRCs and B cells is not as drastic in the Cre+ draining axillary lymph nodes, suggesting that the depletion is not as effective there, but there is still a clear reduction compared to the Cre- draining axillary lymph nodes. Previous published results have ablated the FRCs systemically and only mentioned that local ablation can be achieved (Cremasco et al., 2014; Denton et al., 2014; Novkovic et al., 2016). Even though we used the same protocol that Cremasco et al. (2014) reported to work for local ablation, we could not manage to attain local depletion. This demonstrates that it seems to be difficult to achieve local ablation, and

much optimization needs to be done to accomplish it.

6.5 FRC-depleted lymph node undergoes morphological changes

The Cre+ draining popliteal lymph node undergoes drastic morphological changes during FRC depletion (Figure 13a). The depletion of the FRCs affects the whole lymph node by shrinking, and no structures can be set apart from each other. The B cell follicles lose their boundaries possibly due to the decreased expression of their survival factor BAFF produced by the FRCs. The number of B cells decreases, and the lymphocytes mix throughout the cortex (Cremasco et al., 2014). The toxin-induced death of the CCL19-DTR-expressing cells could also possibly cause inflammatory reactions in the lymph node. Then, the cleaning up of the dead cells through phagocytosis by macrophages could contribute to the overall histological changes, which makes the interpretation of any functional studies difficult. Even though half of the FRC population is ablated, Col I is still present in the lymph node and seems denser compared to the Cre- draining (Figure 13b) and Cre+ non-draining (Figure 13c) popliteal lymph nodes. The cells in the lymph node may compensate for the loss of the FRCs and their contact with neighboring cells by increasing the compactness and surface area in the lymph node. FRCs can fully restore their network after ablation, and it is thought that the regeneration of the FRCs is led by the collagen fibers in the conduit. Therefore, this may be why the collagen remains in the lymph node after depletion (Novkovic et al., 2016). The Cre+ non-draining popliteal lymph node and Cre- draining popliteal lymph node do not undergo FRC depletion, and the morphology seems normal since the different structures in the lymph node can be seen.

6.6 Popliteal lymph node can respond to immunization after FRC depletion

Knowing that the FRCs are important for the structure of the lymph node and regulation of the immune response, we wanted to investigate how the draining lymph node responds to inflammation when the FRC population is reduced. Inflammation was induced in the Cre+ and Cre- FRC-depleted draining popliteal lymph nodes, and the weights were compared to the FRC-depleted popliteal lymph nodes (Figure 14). Since no FRC depletion happens in the Cre- mice, the popliteal lymph node is able to induce an inflammatory response based on the normal expansion of the lymph node. However, the Cre+ popliteal lymph node was also able to expand, but the loss of the FRCs and the B cells diminished the immune response and the expansion of the lymph node. During the first days of acute inflammation, the FRCs stretch, and the extracellular matrix components of the conduit,

e.g., Col I, are reduced by the stretching, and the conduit network is partially disrupted (Denton et al., 2014). The zoom-in of Col I in the inflamed Cre- draining popliteal lymph node (Figure 15b) shows how the Col I fibers are stretched, and the conduit network is sporadic compared to the Cre+ non-draining popliteal lymph node (Figure 15c). Nevertheless, Col I in the inflamed Cre+ draining popliteal lymph node (Figure 15ba) is denser compared to the inflamed Cre- draining and Cre+ non-draining popliteal lymph nodes. One explanation for the dense Col I could be that the remaining 50% of the FRCs try to compensate for the lost FRCs and overproduce Col I to expand the lymph node. The FRCs proliferate during inflammation, and it has been shown that if no mature lymphocytes are available in the lymph node, the FRCs do not survive, and the lymph node expansion is dependent on the lymphocytes (Chyou et al., 2011). Depletion of the FRCs affects the B cell survival, but it also affects the T cells. The adaptive immune response is diminished if $> 50\%$ of the FRCs are lost, which results in the lymphocyte population not expanding (Cremasco et al., 2014; Novkovic et al., 2016). This could explain why the inflamed Cre+ draining popliteal lymph node can increase in size but is not as effective as during normal circumstances.

7 Conclusions

In conclusion, the FRC population can be reduced with a local s.c. injection of DT in the CCL19-iDTR mouse model. The depletion is not local, but most of the depletion of the FRCs occurs in the draining popliteal lymph node. After FRC depletion, the draining popliteal lymph node can respond to immunization even with reduced amounts of FRCs, but not as effectively as during normal circumstances. Based on these results, the FRCs regulate the immune response in the lymph node, but more studies are needed to identify their exact role during inflammation. At the moment, the only way to study the FRCs *in vivo* is with cell type-specific expression of DTR. Depletion of the FRCs *in vivo* can help with the understanding to some extent since the lymph node can only tolerate a reduction of 50% of the FRCs before the function of the lymph node is impaired. More efficient and local genetic tools targeting the FRCs need to be generated to be able to assess their precise function during acute inflammation.

8 Acknowledgements

I would like to express my greatest gratitude to Marko Salmi for the opportunity to immerse myself in immunological research, your insightful comments, and helpful suggestions during my project. I am especially grateful to Ruth Fair-Mäkelä for the excellent supervision and your persistent help with my thesis. I have developed valuable skills from both of you for my future career.

I would also like to thank all the members of Salmi lab for all the scientific and non-scientific talks. A special thank you to my partner Jonatan for your admirable calmness and always listening to me rambling about my project. Finally, I would want to thank my friends and family for supporting me during my time at the university and the whole writing process.

9 Summary in Swedish - Svensk sammanfattning

Reglering av immunsvaret i lymfkörteln med hjälp av de fibroblastiska retikulära cellerna

Introduktion

Det finns flera hundra lymfkörtlar som är sammankopplade runtomkring i människokroppen. Lymfkörtlarnas uppgifter är att initiera ett adaptivt immunsvar mot främmande inkräktare såsom bakterier och virus, och bibehålla självtoleransen mot kroppens egna celler (Choi m.fl. 2012; Girard m.fl. 2012). Lymfkörteln är omgiven av en kapsel av kollagen och består av flera olika strukturella regioner som är cortex, paracortex och medulla. Majoriteten av cellerna i lymfkörtlen är hematopoetiska cellet, medan fem procent av cellerna består av stromaceller. Stromacellerna kan delas in i flera olika undergrupper beroende på deras plats, funktion och fenotyp. Dessa undergrupper är blodkärlsendotelceller, lymfatiska endotelceller och fibroblastiska retikulära celler. Stromacellerna är viktiga för lymfkörtelns funktion eftersom de ger lymfkörteln dess struktur och bidrar i regleringen av immunsvaret (Grasso m.fl. 2021; Jalkanen och Salmi 2020). Det retikulära nätverket produceras av de fibroblastiska retikulära cellerna i lymfkörtelns parenkym. Nätverket består utav flera olika lager, där kärnan utgörs av kollagen typ I och II omgiven av ER-TR7^{+}-mikrofibriller, ett basalmembran och fibroblastiska retikulära celler längst ut. Det retikulära nätverket ger strukturellt stöd åt lymfkörteln och reglerar det storleksselektiva inträdet av antigener i lymfkörteln. Dessutom vägleder det retikulära nätverket migrerande lymfocyter till deras specifika områden i lymfkörteln (Mueller och Germain 2009; Sixt m.fl. 2005). De fibroblastiska retikulära cellerna uttrycker kemokinerna CCL19 och CCL21 som är nödvändiga för migreringen och överlevnaden av lymfocyter och dendritiska celler (Cremasco m.fl. 2014; Luther m.fl. 2000).

Främmande antigener transporteras till lymfkörtlarna under inflammation och det specifika immunförsvaret initieras. De naiva B- och T-cellerna aktiveras efter att de har varit i kontakt med sin specifika antigen, vilket leder till proliferation av lymfocyterna för att hjälpa till med elimineringen av patogenen genom produktion av effektorceller och antikroppar (Batista och Harwood 2009; Groom 2019). Lymfkörteln kan expandera upp till 20-faldigt vid inflammation för att tillgodose inflödet av immunceller, och stromat omformas för att stödja expansionen. Blodkärlsendotelcellerna och de lymfatiska endotelcellerna ökar både i storlek och antal vid inflammation för att underlätta den ökade migrationen av lymfocyter in i parenkymet (Thierry m.fl. 2019). Vid homeostas uttrycker de fibroblastiska retikulära cellerna podoplanin som kontrollerar kontraktionen av akto-

myosin i det retikulära nätverket. Vid inflammation binder CLEC-2 på de dendritiska cellerna till podoplanin, vilket resulterar i att uttrycket av podoplanin blockeras hos de fibroblastiska retikulära cellerna och kontraktionen hämmas. Detta leder till att de fibroblastiska retikulära cellerna slappnar av och det retikulära nätverket sträcks ut, och lymfkörteln kan expandera. De fibroblastiska retikulära cellerna behöver också proliferera för att stromat ska kunna öka i storlek och stödja den växande populationen av lymfocyter (Acton m.fl. 2014; Astarita m.fl. 2015). Efter att patogenen har neutraliserats så drar stromat i lymfkörteln ihop sig och återgår till homeostas (Thierry m.fl. 2019).

CCL19-Cre x iDTR-musmodell använder sig av Cre-loxP rekombineringssystem för att modifiera DNA-sekvensen på ett specifikt ställe i DNA:t. Cre-rekombinaset känner igen loxP-sekvenserna och spjälker DNA-sekvensen mellan loxP-fragmenten. CCL19-Cre-möss (Chai et al., 2013) som uttrycker Cre under *CCL19*-promotorn avlades med iDTR-möss (eng. Cre-inducible diphtheria toxin receptor) (Buch et al., 2005) som uttrycker DTR (eng. diphtheria toxin receptor). Uppfödningen resulterar i möss som bara uttrycker DTR i $CCL19^{+}$-celler hos Cre+-möss (Figur 5). När difteritoxin injiceras i Cre+-möss genomgår de $CCL19^{+}$-cellerna apoptos.

Den första målsättningen med avhandlingen var att etablera en modell där de fibroblastiska retikulära cellerna har lokalt reducerats i de dränerande lymfkörtlarna med CCL19-Cre x iDTR-musmodellen. Den andra målsättningen var att studera hur de dränerande lymfkörtlarna med reducerat antal fibroblastiska retikulära celler reagerar vid inflammation.

I avhandlingen användes två olika musmodeller för att studera de fibroblastiska retikulära cellerna. Flödescytometri användes för att studera cellpopulationerna i lymfkörteln, immunohistokemi för att visualisera lymfkörtlarnas morfologi och slutligen kvantifiering och statistisk analys av erhållna resultat.

Resultat och diskussion

Lokal reducering av de fibroblastiska retikulära cellerna försökte åstadkommas med att injicera subkutant 0,5 ng/g kroppsvikt av difteritoxin en gång i ena foten på bakbenet hos CCL19-iDTR-möss och tre dagar senare skördades lymfkörtlarna (Figur 10a). Cre+-lymfkörtlarna jämfördes med Cre−-lymfkörtlarna eftersom Cre−-lymfkörtlarna inte genomgår någon reducering av de fibriblastiska retikulära cellerna och kan därför användas som negativ kontroll. Det var en signifikant skillnad mellan vikterna på lymfkörtlarna mellan de dränerande lymfkörtlarna i knävecket hos Cre+- och Cre−-möss. Vikten hade minskat med ungefär 50 %, vilket tydde på att en reducering av det totala cellantalet

hade åstadkommits (Figur 10b). Resultaten från flödescytometrin indikerade på att reduceringen av de fibroblastiska retikulära cellerna egentligen inte var lokal utan systemisk, eftersom både procentandelen och cellantalet av de fibroblastiska retikulära cellerna och B-cellerna hade reducerats i lymfkörtlarna i knävecket och armhålan (Figur 11, 12). Reduceringen var effektivast hos de Cre+-dränerande lymfkörtlarna i knävecket men effekten kunde även ses i de dränerande lymfkörtlarna i armhålan och de icke-dränerande lymfkörtlarna i knävecket. Novkovic m.fl. (2016) visade att intraperitoneala injektioner av difteritoxin med en koncentration på 0,5 ng/g kroppsvikt resulterade i måttlig reducering av de fibroblastiska retikulära cellerna och att cellantalet minskade med 37 %. Dessa resultat är i samma linje med resultaten som presenterades i det här forskningsprojektet. Eftersom intraperitoneala injektioner sprider sig över ett större område än subkutana injektioner, får toxinet ett större verkningsområde och lägre effekt på enskilda lymfkörtlar. Den Cre+-dränerande lymfkörteln i knävecket genomgick drastiska morfologiska förändringar under reduceringen av de fibroblastiska retikulära cellerna (Figur 13b). Hela lymfkörteln krympte till följd av reduceringen och lymfocyterna blandas i hela cortex. Kollagen typ I verkade tätare hos den Cre+-dränerande lymfkörteln jämfört med de Cre+-icke-dränerande och Cre−-dränerande lymfkörtlarna. Tidigare studier har visat att de fibroblastiska retikulära cellerna kan helt återställa sitt nätverk efter total reducering och det antas att detta görs med hjälp av kollagen typ I (Novkovic m.fl. 2016). Detta kan vara orsaken till att kollagenet finns kvar i lymfkörteln efter förlusten av de fibroblastiska retikulära cellerna.

Den Cre+-dränerande lymfkörteln i knävecket kunde inte expandera lika effektivt som normalt efter reduceringen av de fibroblastiska retikulära cellerna vid inflammation. Lymfkörteln har endast fördubblat sin vikt medan den inflammerade Cre−-dränerande lymfkörteln i knävecket har ökat sin vikt åttafaldigt (Figur 14b). Resultaten (Figur 15b) påvisar att en inflammation är pågående eftersom att hela den Cre+-dränerande lymfkörteln i knävecket som har injicerats med difteritoxin och komplett Freunds adjuvans har ökat i storlek. Den inflammerade Cre−-dränerande lymfkörteln i knävecket har expanderat som vanligt med förstorade lymfoida folliklar för att motverka inflammationen (Figur 15c). Inzoomningen av kollagen typ I hos den inflammerade Cre+-lymfkörteln i knävecket visar på hur tätt kollagenfibrerna är jämfört med de inflammerade Cre−-dränerande och Cre+-icke-dränerande lymfkörtlarna i knävecket. Reduceringen av de fibroblastiska retikulära cellerna påverkar både B- och T-cellerna, och om minskningen av de fibroblastiska retikulära cellerna är $>$50 % så resulterar det i att lymfocytpopulationen inte ökar (Cremasco m.fl. 2014, Novkovic m.fl. 2016). Detta kan förklara varför den inflammerade Cre+ dränerande lymfkörteln i knävecket kan öka i storlek men inte lika effektivt som under

normala förhållanden.

Sammanfattningsvis så kan omkring hälften av de fibroblastiska retikulära cellerna reduceras med hjälp av difteritoxin i CCL19-iDTR-musmodellen. Reduceringen är systemisk men den största reduceringen kan ses i de Cre+-lymfkörtlarna i knävecket. Den Cre+-dränerande lymfkörteln i knävecket kan expandera vid inflammation efter reducering av de fibroblastiska retikulära cellerna men expanderingen är inte lika effektiv som vid normala förhållanden. På basis av dessa resultat så visas det att de fibroblastiska retikulära cellerna reglerar immunsvaret, men fortsatta studier krävs för att kunna identifiera exakt hur de reglerar immunsvaret.

References

Acton, S. E., Astarita, J. L., Malhotra, D., Lukacs-Kornek, V., Franz, B., Hess, P. R., ... Turley, S. J. (2012). Podoplanin-rich stromal networks induce dendritic cell motility via activation of the C-type lectin receptor CLEC-2. *Immunity*, *37*(2), 276–289.

Acton, S. E., Farrugia, A. J., Astarita, J. L., á, D., Jenkins, R. P., Nye, E., ... Reis e Sousa, C. (2014). Dendritic cells control fibroblastic reticular network tension and lymph node expansion. *Nature*, *514*(7523), 498–502.

Acton, S. E., & Reis e Sousa, C. (2016). Dendritic cells in remodeling of lymph nodes during immune responses. *Immunol. Rev.*, *271*(1), 221–229.

Angeli, V., Ginhoux, F., à, J., Quemeneur, L., Frenette, P. S., Skobe, M., ... Randolph, G. J. (2006). B cell-driven lymphangiogenesis in inflamed lymph nodes enhances dendritic cell mobilization. *Immunity*, *24*(2), 203–215.

Ansel, K. M., Ngo, V. N., Hyman, P. L., Luther, S. A., rster, R., Sedgwick, J. D., ... Cyster, J. G. (2000). A chemokine-driven positive feedback loop organizes lymphoid follicles. *Nature*, *406*(6793), 309–314.

Astarita, J. L., Cremasco, V., Fu, J., Darnell, M. C., Peck, J. R., Nieves-Bonilla, J. M., ... Turley, S. J. (2015). The CLEC-2-podoplanin axis controls the contractility of fibroblastic reticular cells and lymph node microarchitecture. *Nat. Immunol.*, *16*(1), 75–84.

Bajénoff, M., Egen, J. G., Koo, L. Y., Laugier, J. P., Brau, F., Glaichenhaus, N., & Germain, R. N. (2006). Stromal cell networks regulate lymphocyte entry, migration, and territoriality in lymph nodes. *Immunity*, *25*(6), 989–1001.

Baptista, A. P., Roozendaal, R., Reijmers, R. M., Koning, J. J., Unger, W. W., Greuter, M., ... Mebius, R. E. (2014). Lymph node stromal cells constrain immunity via MHC class II self-antigen presentation. *Elife*, *3*, e04433.

Baratin, M., Simon, L., Jorquera, A., Ghigo, C., Dembele, D., Nowak, J., ... Bajénoff, M. (2017). T Cell Zone Resident Macrophages Silently Dispose of Apoptotic Cells in the Lymph Node. *Immunity*, *47*(2), 349–362.

Batista, F., & Harwood, N. (2009). The who, how and where of antigen presentation to B cells. *Nat. Rev. Immunol.*, *9*, 15–27.

Bellomo, A., Gentek, R., Bajénoff, M., & Baratin, M. (2018). Lymph node macrophages: Scavengers, immune sentinels and trophic effectors. *Cell Immunol.*, *330*, 168–174.

Benahmed, F., Chyou, S., Dasoveanu, D., Chen, J., Kumar, V., Iwakura, Y., & Lu, T. T. (2014). Multiple CD11+ cells collaboratively express IL-1β to modulate stromal vascular endothelial growth factor and lymph node vascular-stromal growth. *J Immunol*, *192*(9), 4153–4163.

Berg, E. L., McEvoy, L. M., Berlin, C., Bargatze, R. F., & Butcher, E. C. (1993). L-selectin-mediated lymphocyte rolling on MAdCAM-1. *Nature*, *366*(6456), 695–

698.

Braun, A., Worbs, T., Moschovakis, G. L., Halle, S., Hoffmann, K., lter, J., ... Förster, R. (2011). Afferent lymph-derived T cells and DCs use different chemokine receptor CCR7-dependent routes for entry into the lymph node and intranodal migration. *Nat. Immunol.*, *12*(9), 879–887.

Buch, T., Heppner, F. L., Tertilt, C., Heinen, T. J., Kremer, M., Wunderlich, F. T., ... Waisman, A. (2005). A cre-inducible diphtheria toxin receptor mediates cell lineage ablation after toxin administration. *Nature Methods*, *2*.

Chai, Q., Onder, L., Scandella, E., Gil-Cruz, C., Perez-Shibayama, C., Cupovic, J., ... Ludewig, B. (2013). Maturation of lymph node fibroblastic reticular cells from myofibroblastic precursors is critical for antiviral immunity. *Immunity*, *38*(5), 1013–1024.

Choi, I., Lee, S., & Hong, Y. K. (2012). The new era of the lymphatic system: No longer secondary to the blood vascular system. *Cold Spring Harbor Perspectives in Medicine*, *2*.

Chyou, S., Benahmed, F., Chen, J., Kumar, V., Tian, S., Lipp, M., & Lu, T. T. (2011). Coordinated regulation of lymph node vascular-stromal growth first by CD11c+ cells and then by T and B cells. *J. Immunol.*, *187*(11), 5558–5567.

Chyou, S., Ekland, E. H., Carpenter, A. C., Tzeng, T. C., Tian, S., Michaud, M., ... Lu, T. T. (2008). Fibroblast-type reticular stromal cells regulate the lymph node vasculature. *J. Immunol.*, *181*(6), 3887–3896.

Cohen, J. N., Guidi, C. J., Tewalt, E. F., Qiao, H., Rouhani, S. J., Ruddell, A., ... Engelhard, V. H. (2010). Lymph node-resident lymphatic endothelial cells mediate peripheral tolerance via Aire-independent direct antigen presentation. *J. Exp. Med.*, *207*(4), 681–688.

Cremasco, V., Woodruff, M. C., Onder, L., Cupovic, J., Nieves-Bonilla, J. M., Schildberg, F. A., ... Turley, S. J. (2014). B cell homeostasis and follicle confines are governed by fibroblastic reticular cells. *Nat. Immunol.*, *15*(10), 973–981.

Cyster, J. G., & Schwab, S. R. (2012). Sphingosine-1-phosphate and lymphocyte egress from lymphoid organs. *Annu. Rev. Immunol.*, *30*, 69–94.

Denton, A. E., Roberts, E. W., Linterman, M. A., & Fearon, D. T. (2014). Fibroblastic reticular cells of the lymph node are required for retention of resting but not activated CD8+ T cells. *Proc. Natl. Acad. Sci. U.S.A.*, *111*(33), 12139–12144.

Dubrot, J., Duraes, F. V., Potin, L., Capotosti, F., Brighouse, D., Suter, T., ... Hugues, S. (2014). Lymph node stromal cells acquire peptide-MHCII complexes from dendritic cells and induce antigen-specific $CD4^+$ T cell tolerance. *J. Exp. Med.*, *211*(6), 1153–1166.

Duckworth, B. C., & Groom, J. R. (2021). Conversations that count: Cellular interactions that drive T cell fate. *Immunol. Rev.*, *300*(1), 203–219.

Fletcher, A. L., Lukacs-Kornek, V., Reynoso, E. D., Pinner, S. E., Bellemare-Pelletier, A., Curry, M. S., ... Turley, S. J. (2010). Lymph node fibroblastic reticular cells directly present peripheral tissue antigen under steady-state and inflammatory conditions. *J. Exp. Med.*, *207*(4), 689–697.

Fujimoto, N., He, Y., D'Addio, M., Tacconi, C., Detmar, M., & Dieterich, L. C. (2020). Single-cell mapping reveals new markers and functions of lymphatic endothelial cells in lymph nodes. *PLoS Biol.*, *18*(4), e3000704.

Förster, R., Schubel, A., Breitfeld, D., Kremmer, E., ller, I., Wolf, E., & Lipp, M. (1999). CCR7 coordinates the primary immune response by establishing functional microenvironments in secondary lymphoid organs. *Cell*, *99*(1), 23–33.

Garside, P., Ingulli, E., Merica, R. R., Johnson, J. G., Noelle, R. J., & Jenkins, M. K. (1998). Visualization of specific B and T lymphocyte interactions in the lymph node. *Science*, *281*(5373), 96–99.

Gerner, M. Y., Kastenmuller, W., Ifrim, I., Kabat, J., & Germain, R. N. (2012). Histocytometry: a method for highly multiplex quantitative tissue imaging analysis applied to dendritic cell subset microanatomy in lymph nodes. *Immunity*, *37*(2), 364–376.

Girard, J. P., Moussion, C., & Förster, R. (2012). HEVs, lymphatics and homeostatic immune cell trafficking in lymph nodes. *Nat. Rev. Immunol.*, *12*(11), 762–773.

Girard, J. P., & Springer, T. A. (1995). High endothelial venules (HEVs): specialized endothelium for lymphocyte migration. *Immunol. Today*, *16*(9), 449–457.

Grasso, C., Pierie, C., Mebius, R. E., & van Baarsen, L. G. M. (2021). Lymph node stromal cells: subsets and functions in health and disease. *Trends. Immunol.*, *42*(10), 920–936.

Gray, E. E., & Cyster, J. G. (2012). Lymph node macrophages. *J. Innate Immun.*, *4*(5-6), 424–436.

Gregory, J. L., Walter, A., Alexandre, Y. O., Hor, J. L., Liu, R., Ma, J. Z., ... Mueller, S. N. (2017). Infection Programs Sustained Lymphoid Stromal Cell Responses and Shapes Lymph Node Remodeling upon Secondary Challenge. *Cell Rep.*, *18*(2), 406–418.

Gretz, J. E., Norbury, C. C., Anderson, A. O., Proudfoot, A. E., & Shaw, S. (2000). Lymph-borne chemokines and other low molecular weight molecules reach high endothelial venules via specialized conduits while a functional barrier limits access to the lymphocyte microenvironments in lymph node cortex. *J. Exp. Med.*, *192*(10), 1425–1440.

Groom, J. R. (2019). Regulators of T-cell fate: Integration of cell migration, differentiation and function. *Immunol. Rev.*, *289*(1), 101–114.

Gunn, M. D., Ngo, V. N., Ansel, K. M., Ekland, E. H., Cyster, J. G., & Williams, L. T. (1998). A B-cell-homing chemokine made in lymphoid follicles activates Burkitt's

lymphoma receptor-1. *Nature*, *391*(6669), 799–803.

Harrell, M. I., Iritani, B. M., & Ruddell, A. (2008). Lymph node mapping in the mouse. *J. Immunol. Methods*, *332*(1-2), 170–174.

Hayakawa, M., Kobayashi, M., & Hoshino, T. (1988). Direct contact between reticular fibers and migratory cells in the paracortex of mouse lymph nodes: a morphological and quantitative study. *Arch. Histol. Cytol.*, *51*(3), 233–240.

Hayashi, S., Tenzen, T., & McMahon, A. P. (2003). Maternal inheritance of Cre activity in a Sox2Cre deleter strain. *Genesis*, *37*(2), 51–53.

Heffner, C. S., Herbert Pratt, C., Babiuk, R. P., Sharma, Y., Rockwood, S. F., Donahue, L. R., … Murray, S. A. (2012). Supporting conditional mouse mutagenesis with a comprehensive cre characterization resource. *Nat. Commun.*, *3*, 1218.

Herzog, B. H., Fu, J., Wilson, S. J., Hess, P. R., Sen, A., McDaniel, J. M., … Xia, L. (2013). Podoplanin maintains high endothelial venule integrity by interacting with platelet CLEC-2. *Nature*, *502*(7469), 105–109.

Hirosue, S., & Dubrot, J. (2015). Modes of Antigen Presentation by Lymph Node Stromal Cells and Their Immunological Implications. *Front. Immunol.*, *6*, 446.

Hunter, M. C., Teijeira, A., & Halin, C. (2016). T Cell Trafficking through Lymphatic Vessels. *Front. Immunol.*, *7*, 613.

Itano, A. A., & Jenkins, M. K. (2003). Antigen presentation to naive CD4 T cells in the lymph node. *Nat. Immunol.*, *4*(8), 733–739.

Itano, A. A., McSorley, S. J., Reinhardt, R. L., Ehst, B. D., Ingulli, E., Rudensky, A. Y., & Jenkins, M. K. (2003). Distinct dendritic cell populations sequentially present antigen to CD4 T cells and stimulate different aspects of cell-mediated immunity. *Immunity*, *19*(1), 47–57.

Jalkanen, S., & Salmi, M. (2020). Lymphatic endothelial cells of the lymph node. *Nat. Rev. Immunol.*, *20*(9), 566–578.

Junt, T., Moseman, E. A., Iannacone, M., Massberg, S., Lang, P. A., Boes, M., … von Andrian, U. H. (2007). Subcapsular sinus macrophages in lymph nodes clear lymph-borne viruses and present them to antiviral B cells. *Nature*, *450*(7166), 110–114.

Katakai, T. (2012). Marginal reticular cells: a stromal subset directly descended from the lymphoid tissue organizer. *Front. Immunol.*, *3*, 200.

Katakai, T., Hara, T., Lee, J. H., Gonda, H., Sugai, M., & Shimizu, A. (2004). A novel reticular stromal structure in lymph node cortex: an immuno-platform for interactions among dendritic cells, T cells and B cells. *Int. Immunol.*, *16*(8), 1133–1142.

Kim, J., Koo, B. K., & Knoblich, J. A. (2020). Human organoids: model systems for human biology and medicine. *Nat. Rev. Mol. Cell Biol.*, *21*(10), 571–584.

Kumar, V., Dasoveanu, D. C., Chyou, S., Tzeng, T. C., Rozo, C., Liang, Y., … Lu, T. T. (2015). A dendritic-cell-stromal axis maintains immune responses in lymph nodes. *Immunity*, *42*(4), 719–730.

Kähäri, L., Fair-Mäkelä, R., Auvinen, K., Rantakari, P., Jalkanen, S., Ivaska, J., & Salmi, M. (2019). Transcytosis route mediates rapid delivery of intact antibodies to draining lymph nodes. *J. Clin. Invest.*, *129*(8), 3086–3102.

Li, L., Wu, J., Abdi, R., Jewell, C. M., & Bromberg, J. S. (2021). Lymph node fibroblastic reticular cells steer immune responses. *Trends. Immunol.*, *42*(8), 723–734.

Liao, S., & Ruddle, N. H. (2006). Synchrony of high endothelial venules and lymphatic vessels revealed by immunization. *J. Immunol.*, *177*(5), 3369–3379.

Link, A., Vogt, T. K., Favre, S., Britschgi, M. R., Acha-Orbea, H., Hinz, B., ... Luther, S. A. (2007). Fibroblastic reticular cells in lymph nodes regulate the homeostasis of naive T cells. *Nat. Immunol.*, *8*(11), 1255–1265.

Liston, A., Kohler, R. E., Townley, S., Haylock-Jacobs, S., Comerford, I., Caon, A. C., ... McColl, S. R. (2009). Inhibition of CCR6 function reduces the severity of experimental autoimmune encephalomyelitis via effects on the priming phase of the immune response. *J. Immunol.*, *182*(5), 3121–3130.

Luther, S. A., Tang, H. L., Hyman, P. L., Farr, A. G., & Cyster, J. G. (2000). Coexpression of the chemokines ELC and SLC by T zone stromal cells and deletion of the ELC gene in the *plt*/*plt* mouse. *Proc. Natl. Acad. Sci. U.S.A.*, *97*(23), 12694–12699.

Lämmermann, T., Bader, B. L., Monkley, S. J., Worbs, T., ldner, R., Hirsch, K., ... Sixt, M. (2008). Rapid leukocyte migration by integrin-independent flowing and squeezing. *Nature*, *453*(7191), 51–55.

Lütge, M., Pikor, N. B., & Ludewig, B. (2021). Differentiation and activation of fibroblastic reticular cells. *Immunol. Rev.*, *302*(1), 32–46.

Mackay, C. R., Marston, W. L., & Dudler, L. (1990). Naive and memory T cells show distinct pathways of lymphocyte recirculation. *J. Exp. Med.*, *171*(3), 801–817.

MacLennan, I. C., Gulbranson-Judge, A., Toellner, K. M., Casamayor-Palleja, M., Chan, E., Sze, D. M., ... Orbea, H. A. (1997). The changing preference of T and B cells for partners as T-dependent antibody responses develop. *Immunol. Rev.*, *156*, 53–66.

Malhotra, D., Fletcher, A. L., Astarita, J., Lukacs-Kornek, P., V.and Tayalia, Gonzalez, S. F., Elpek, K. G., ... Consortium, I. G. P. (2012). Transcriptional profiling of stroma from inflamed and resting lymph nodes defines immunological hallmarks. *Nat. Immunol.*, *13*(5), 499–510.

Malhotra, D., Fletcher, A. L., & Turley, S. J. (2013). Stromal and hematopoietic cells in secondary lymphoid organs: partners in immunity. *Immunol. Rev.*, *251*(1), 160–176.

Martinez, V. G., Pankova, V., Krasny, L., Singh, T., Makris, S., White, I. J., ... Acton, S. E. (2019). Fibroblastic Reticular Cells Control Conduit Matrix Deposition during Lymph Node Expansion. *Cell Rep.*, *29*(9), 2810–2822.

Masopust, D., Sivula, C. P., & Jameson, S. C. (2017). Of Mice, Dirty Mice, and Men:

Using Mice To Understand Human Immunology. *J. Immunol.*, *199*(2), 383–388.

Moore Jr., J. E., & Bertram, C. D. (2018). Lymphatic System Flows. *Annu. Rev. Fluid. Mech.*, *50*, 459–482.

Moussion, C., & Girard, J. P. (2011). Dendritic cells control lymphocyte entry to lymph nodes through high endothelial venules. *Nature*, *479*(7374), 542–546.

Mueller, S. N., & Germain, R. N. (2009). Stromal cell contributions to the homeostasis and functionality of the immune system. *Nat. Rev. Immunol.*, *9*(9), 618–629.

Nadafi, R., a, C., Keuning, E. D., Koning, J. J., de Kivit, S., Konijn, T., … Mebius, R. E. (2020). Lymph Node Stromal Cells Generate Antigen-Specific Regulatory T Cells and Control Autoreactive T and B Cell Responses. *Cell Rep.*, *30*(12), 4110–4123.

Novkovic, M., Onder, L., Cupovic, J., Abe, J., Bomze, D., Cremasco, V., … Ludewig, B. (2016). Topological Small-World Organization of the Fibroblastic Reticular Cell Network Determines Lymph Node Functionality. *PLoS Biol.*, *14*(7), e1002515.

Okada, T., Miller, M. J., Parker, I., Krummel, M. F., Neighbors, M., Hartley, S. B., … Cyster, J. G. (2005). Antigen-engaged B cells undergo chemotaxis toward the T zone and form motile conjugates with helper T cells. *PLoS Biol.*, *3*(6), e150.

Park, C., Hwang, I. Y., Sinha, R. K., Kamenyeva, O., Davis, M. D., & Kehrl, J. H. (2012). Lymph node B lymphocyte trafficking is constrained by anatomy and highly dependent upon chemoattractant desensitization. *Blood*, *119*(4), 978–989.

Perez-Shibayama, C., Gil-Cruz, C., & Ludewig, B. (2019). Fibroblastic reticular cells at the nexus of innate and adaptive immune responses. *Immunological reviews*, *289*(1), 31–41.

Pham, T. H., Okada, T., Matloubian, M., Lo, C. G., & Cyster, J. G. (2008). S1P1 receptor signaling overrides retention mediated by Gα_i-coupled receptors to promote T cell egress. *Immunity*, *28*(1), 122–133.

Phan, T. G., Green, J. A., Gray, E. E., Xu, Y., & Cyster, J. G. (2009). Immune complex relay by subcapsular sinus macrophages and noncognate B cells drives antibody affinity maturation. *Nat. Immunol.*, *10*(7), 786–793.

Phan, T. G., Grigorova, I., Okada, T., & Cyster, J. G. (2007). Subcapsular encounter and complement-dependent transport of immune complexes by lymph node B cells. *Nat. Immunol.*, *8*(9), 992–1000.

Randolph, G. J., Angeli, V., & Swartz, M. A. (2005). Dendritic-cell trafficking to lymph nodes through lymphatic vessels. *Nat. Rev. Immunol.*, *5*(8), 617–628.

Randolph, G. J., Ivanov, S., Zinselmeyer, B. H., & Scallan, J. P. (2017). The lymphatic system: Integral roles in immunity. *Annu. Rev. Immunol.*, *35*, 31–52.

Rantakari, P., Auvinen, K., Jäppinen, N., Kapraali, M., Valtonen, J., Karikoski, M., … Salmi, M. (2015). The endothelial protein PLVAP in lymphatics controls the entry of lymphocytes and antigens into lymph nodes. *Nat. Immunol.*, *16*(4), 386–396.

Reith, W., LeibundGut-Landmann, S., & Waldburger, J. M. (2005). Regulation of MHC

class II gene expression by the class II transactivator. *Nat. Rev. Immunol.*, *5*(10), 793–806.

Rodda, L. B., Lu, E., Bennett, M. L., Sokol, C. L., Wang, X., Luther, S. A., ... Cyster, J. G. (2018). Single-Cell RNA Sequencing of Lymph Node Stromal Cells Reveals Niche-Associated Heterogeneity. *Immunity*, *48*(5), 1014–1028.

Roozendaal, R., Mempel, T. R., Pitcher, L. A., Gonzalez, S. F., Verschoor, A., Mebius, R. E., ... Carroll, M. C. (2009). Conduits mediate transport of low-molecular-weight antigen to lymph node follicles. *Immunity*, *30*(2), 264–276.

Rouhani, S. J., Eccles, J. D., Riccardi, P., Peske, J. D., Tewalt, E. F., Cohen, J. N., ... Engelhard, V. H. (2015). Roles of lymphatic endothelial cells expressing peripheral tissue antigens in CD4 T-cell tolerance induction. *Nat. Commun.*, *6*, 6771.

Schiavinato, A., Przyklenk, M., Kobbe, B., Paulsson, M., & Wagener, R. (2021). Collagen type VI is the antigen recognized by the ER-TR7 antibody. *Eur J Immunol*, *51*(9), 2345–2347.

Sixt, M., Kanazawa, N., Selg, M., Samson, T., Roos, G., Reinhardt, D. P., ... Sorokin, L. (2005). The conduit system transports soluble antigens from the afferent lymph to resident dendritic cells in the T cell area of the lymph node. *Immunity*, *22*(1), 19–29.

Soderberg, K. A., Payne, G. W., Sato, A., Medzhitov, R., Segal, S. S., & Iwasaki, A. (2005). Innate control of adaptive immunity via remodeling of lymph node feed arteriole. *Proc. Natl. Acad. Sci. U.S.A.*, *102*(45), 16315–16320.

Streeter, P. R., Rouse, B. T., & Butcher, E. C. (1988). Immunohistologic and functional characterization of a vascular addressin involved in lymphocyte homing into peripheral lymph nodes. *J. Cell Biol.*, *107*(5), 1853–1862.

Takeda, A., Hollmén, M., Dermadi, D., Pan, J., Brulois, K. F., Kaukonen, R., ... Jalkanen, S. (2019). Single-Cell Survey of Human Lymphatics Unveils Marked Endothelial Cell Heterogeneity and Mechanisms of Homing for Neutrophils. *Immunity*, *51*(3), 561–572.

Tewalt, E. F., Cohen, J. N., Rouhani, S. J., Guidi, C. J., Qiao, H., Fahl, S. P., ... Engelhard, V. H. (2012). Lymphatic endothelial cells induce tolerance via PD-L1 and lack of costimulation leading to high-level PD-1 expression on CD8 T cells. *Blood*, *120*(24), 4772–4782.

Thierry, G. R., Gentek, R., & Bajénoff, M. (2019). Remodeling of reactive lymph nodes: Dynamics of stromal cells and underlying chemokine signaling. *Immunol. Rev.*, *289*(1), 42–61.

Ulvmar, M. H., Werth, K., Braun, A., Kelay, P., Hub, E., Eller, K., ... Rot, A. (2014). The atypical chemokine receptor CCRL1 shapes functional CCL21 gradients in lymph nodes. *Nat. Immunol.*, *15*(7), 623–630.

Veerman, K., Tardiveau, C., Martins, F., Coudert, J., & Girard, J. P. (2019). Single-

Cell Analysis Reveals Heterogeneity of High Endothelial Venules and Different Regulation of Genes Controlling Lymphocyte Entry to Lymph Nodes. *Cell Rep.*, *26*(11), 3116–3131.

Vella, G., Guelfi, S., & Bergers, G. (2021). High Endothelial Venules: A Vascular Perspective on Tertiary Lymphoid Structures in Cancer. *Front. Immunol.*, *12*, 736670.

Webster, B., Ekland, E. H., Agle, L. M., Chyou, S., Ruggieri, R., & Lu, T. T. (2006). Regulation of lymph node vascular growth by dendritic cells. *J. Exp. Med.*, *203*(8), 1903–1913.

Worbs, T., Hammerschmidt, S. I., & Förster, R. (2017). Dendritic cell migration in health and disease. *Nat. Rev. Immunol.*, *17*(1), 30–48.

Worbs, T., Mempel, T. R., lter, J., von Andrian, U. H., & rster, R. (2007). CCR7 ligands stimulate the intranodal motility of T lymphocytes in vivo. *J. Exp. Med.*, *204*(3), 489–495.

Xiang, M., Grosso, R. A., Takeda, A., Pan, J., Bekkhus, T., Brulois, K., … Butcher, E. C. (2020). A Single-Cell Transcriptional Roadmap of the Mouse and Human Lymph Node Lymphatic Vasculature. *Front. Cardiovasc. Med.*, *7*, 52.

Yang, C. Y., Vogt, T. K., Favre, S., Scarpellino, L., Huang, H. Y., Tacchini-Cottier, F., & Luther, S. A. (2014). Trapping of naive lymphocytes triggers rapid growth and remodeling of the fibroblast network in reactive murine lymph nodes. *Proc. Natl. Acad. Sci. U.S.A.*, *111*(1), E109–118.

Appendix

A

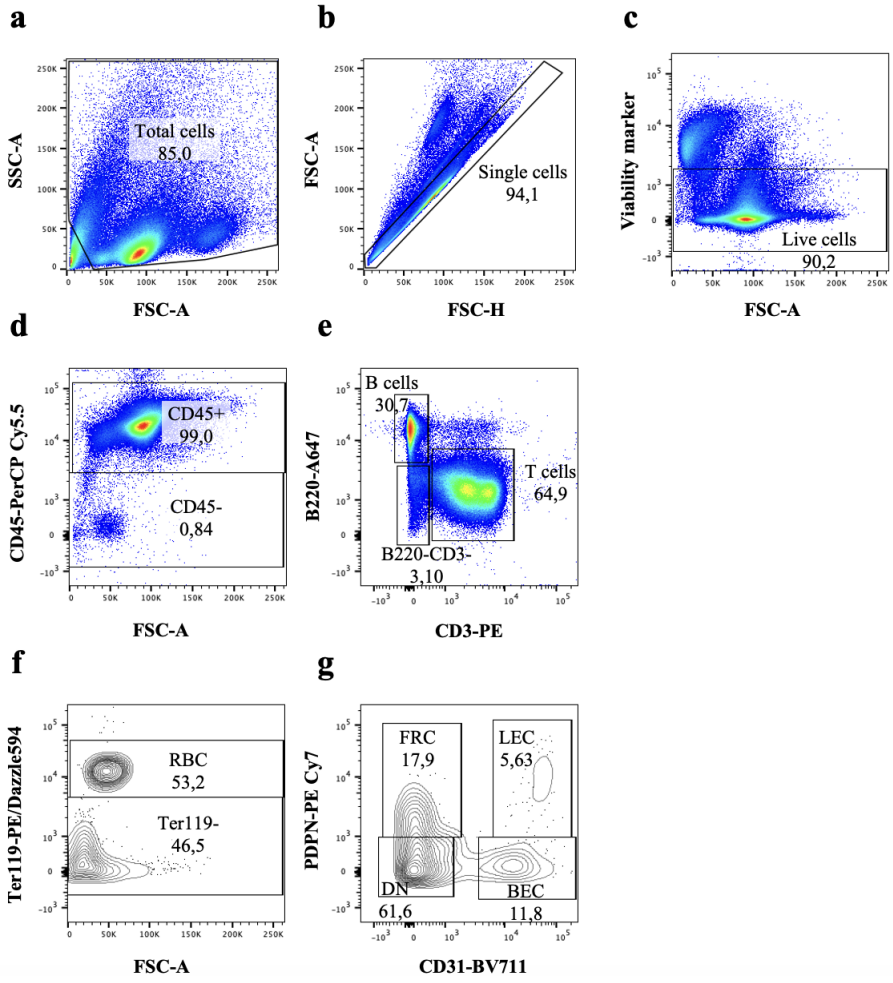

Figure A.1. Gating strategy for sorting the stromal cells in FlowJo software. **a**, Total cells were gated in a dot plot based on the cell size and granularity excluding debris from the acquired data. **b**, A new dot plot was created to eliminate doublets, with the FSH-H on the x-axis and FSH-A on the y-axis from the total cell population. **c**, To exclude all dead cells a new dot plot was created from the single cell plot, where the live cells were gated using the intensity of the viability marker versus cell size. **d**, $CD45^+$ lymphocytes and $CD45^-$ cells were visualized and gated from the live cell population. **e**, A new dot plot consisting of B cell and T cell populations was created from the $CD45^+$ population with B220-A647 on the y-axis and CD3-PE on the x-axis. **f**, $Ter119^+$ red blood cells and $Ter119^-$ cells could be gated from $CD45^-$ negative cells from the intensity of Ter119 versus cell size. **g**, The stromal cell populations, including FRCs ($PDPN^+$, $CD31^-$), LECs ($PDPN^+$, $CD31^+$), BECs ($PDPN^-$, $CD31^+$), and DNs ($PDPN^-$, $CD31^-$) were gated using the intensity of PDPN versus CD31 from the $Ter119^-$ cell population. Values show percentages.